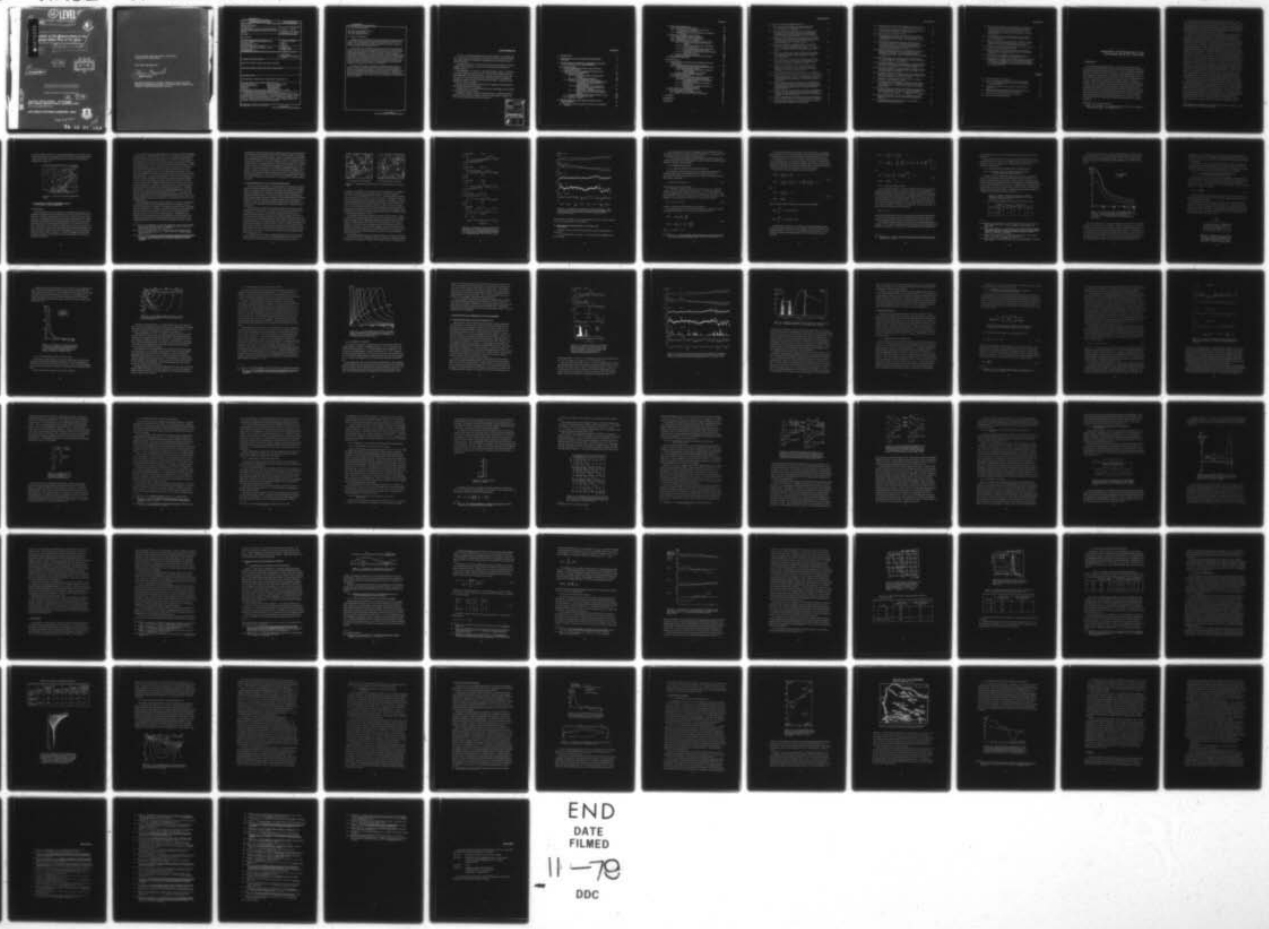
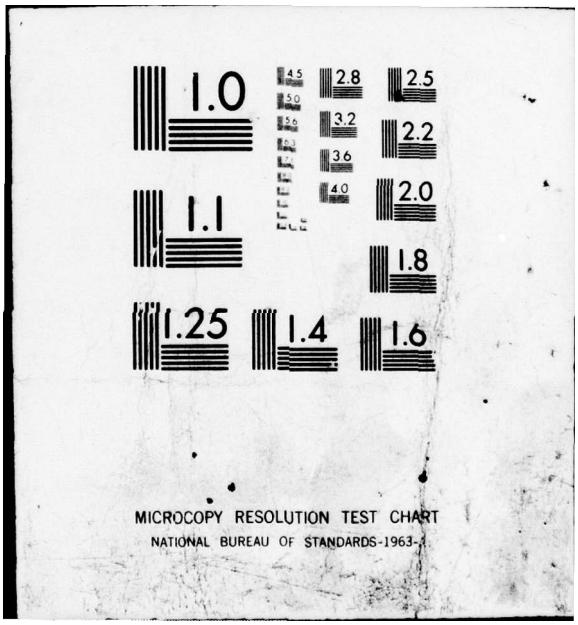
AD-A074 525 AIR FORCE GEOPHYSICS LAB HANSCOM AFB MA F/G 8/7
INTERPRETATION OF TILT MEASUREMENTS IN THE PERIOD RANGE ABOVE T--ETC(U)
APR 79 K HERBST
UNCLASSIFIED AFGL-TR-79-0093 NL

1 OF
AD
A074525



END
DATE
FILMED
11-79
DDC


1.0
1.1
1.25
1.4
1.6
1.8
2.0
2.2
2.5
2.8
3.2
3.6
4.0
4.5
5.0
5.6
MICROCOPY RESOLUTION TEST CHART
NATIONAL BUREAU OF STANDARDS-1963-A

(12) LEVEL II

(14) -9093, AFBL-TRANS-149

AD A074525

...etation of Tilt Measurements in the ... Range Above That of the Tides.

(9) Interim rept.,

...SST

(12) 92

DDC RECEIVED OCT 2 1979 B

(11) 25 April 1979

Approved for public release; distribution unlimited.

DDC FILE COPY

Translated by K. Bennett Howe, International Translation Co.

(16) (17) 10

TERRESTRIAL SCIENCES DIVISION PROJECT 7600

AIR FORCE GEOPHYSICS LABORATORY

HANSCOM AFB, MASSACHUSETTS 01731

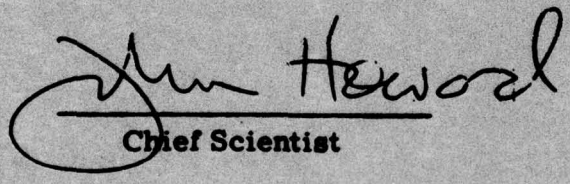
AIR FORCE SYSTEMS COMMAND, USAF

409578

79 10 01 104

This technical report has been reviewed and
is approved for publication.

FOR THE COMMANDER



Chief Scientist

Qualified requestors may obtain additional copies from the
Defense Documentation Center. All others should apply to the
National Technical Information Service.

Unclassified

SECURITY CLASSIFICATION OF THIS PAGE (When Data Entered)

REPORT DOCUMENTATION PAGE		READ INSTRUCTIONS BEFORE COMPLETING FORM
1. REPORT NUMBER AFGL-TR-79-0093	2. GOVT ACCESSION NO.	3. RECIPIENT'S CATALOG NUMBER
4. TITLE (and Subtitle) INTERPRETATION OF TILT MEASUREMENTS IN THE PERIOD RANGE ABOVE THAT OF THE TIDES		5. TYPE OF REPORT & PERIOD COVERED Scientific. Interim. 6. PERFORMING ORG. REPORT NUMBER Translations, No. 109
7. AUTHOR(s) Klaus Herbst		8. CONTRACT OR GRANT NUMBER(s)
9. PERFORMING ORGANIZATION NAME AND ADDRESS Air Force Geophysics Laboratory (LWH) Hanscom AFB Massachusetts 01731		10. PROGRAM ELEMENT, PROJECT, TASK AREA & WORK UNIT NUMBERS 62101F 76001001
11. CONTROLLING OFFICE NAME AND ADDRESS Air Force Geophysics Laboratory (LWH) Hanscom AFB Massachusetts 01731		12. REPORT DATE 25 April 1979 13. NUMBER OF PAGES 89
14. MONITORING AGENCY NAME & ADDRESS(if different from Controlling Office)		15. SECURITY CLASS. (of this report) Unclassified 15a. DECLASSIFICATION/DOWNGRADING SCHEDULE

16. DISTRIBUTION STATEMENT (of this Report)

Approved for public release; distribution unlimited.

17. DISTRIBUTION STATEMENT (of the abstract entered in Block 20, if different from Report)

18. SUPPLEMENTARY NOTES

Translated by K. Bennett Howe, International Translation Co.

19. KEY WORDS (Continue on reverse side if necessary and identify by block number)

Borehole tiltmeters	Maximum entropy method
Finite element method	Earth deformation
Earth tilt	Askania tiltmeter
Tiltmeters	Long-period tilt
Hartz Mountains (West Germany)	Atmospheric pressure loading

20. ABSTRACT (Continue on reverse side if necessary and identify by block number)

Earth tilts were measured at the Zellerfeld-Mühlenhöhe station in the Hartz Mountains, West Germany, for 2-1/2 years from 1972 to 1974. Askania borehole tiltmeters were emplaced in fractured graywacke at depths of 15 m and 30 m with a horizontal separation of 15 m. Tilts at periods greater than tidal were analyzed in terms of the effects of surface loading, temperature variations, precipitation, and tectonic deformation.

DD FORM 1 JAN 73 1473 EDITION OF 1 NOV 65 IS OBSOLETE

Unclassified

SECURITY CLASSIFICATION OF THIS PAGE (When Data Entered)

19. Key Words (Continued)

Tilts from meteorological effects
Tilts from loading effects
Tilts from topographic effects

20. Abstract (Continued)

Both theoretical calculations and experimental results showed that the tilt variations caused by atmospheric pressure changes loading the earth's surface were considerably less than 50 nanoradians even for a low of 899 mb. The poor signal:noise ratio caused by precipitation did not allow further investigation of this phenomenon.

The dominant tilts at periods of several days were caused by penetration of water from rain or melting snow into the ground. It could be shown that the process could not be explained in terms of a simple linear model relating precipitation and tilt, nor by simple but reasonable models of thermoelastic distortion, clay mineral expansion, surface loading, or water level changes in a weak layer. These tilts could, however, be successfully modeled in terms of lateral fluctuations of water level in the vertical fractures in the graywacke caused by variations in overburden thickness. The resulting pressure differences caused elastic bending of the rock between adjacent fractures. This model was a good agreement with the observed amplitudes, amplitude ratio, direction, and timing.

An annual tilt component was identified with the maximum entropy method. Model calculation with the finite element method showed that the tilts were caused by strain induced by coupling of the thermal boundary layer with the undulating topography. It was not possible to separate installation or instrumental effects from possible tectonic tilts, although both instruments did show a net tilt downward to the northeast, a direction approximately perpendicular to the strike of the major mineralized veins and fractures in the region.

Acknowledgments

Prof. Dr. O. Rosenbach deserves my particular thanks for his valuable support, in particular for his expertise, which made it possible to finance this study from a grant based on the Graduate Encouragement Law, as well as for supervision of this study.

I gratefully thank Prof. W. Torge for his interest in this study and for encouraging it with his expertise, as well as for taking on the job of associate or assistant reporter.

My colleagues Dr. D. Flach, W. Grosse-Brauckmann, and Dr. G. Jentzsch have made a significant contribution to this work with their continuous interest, many suggestions, and critical comments. Significant contributions came from Prof. Dr. J. C. Harrison during his stay at the local Institute for Geophysics, especially in regard to the use of the finite element method. I thank all of them sincerely for their great support.

Further, all my colleagues at the Institute for Geophysics who advised me in detailed questions deserve my thanks.

I thank the staff of the German Weather Service in Braunlage for their support in preparing observation material.

In addition, I thank the staff of the Computer Center of Clausthal Technical University and the Regional Computer Center for Niedersachsen, Hannover, for their aid in carrying out the extensive calculations.

ACCESSION for
NTIS White Section ☑
DDC Buff Section ☐
UNANNOUNCED ☐
JUSTIFICATION
BY
DISTRIBUTION/AVAILABILITY CODES
Dist. AVAIL. and/or SPECIAL
A

Contents

1. INTRODUCTION 11

2. DESCRIPTION OF THE ZELLERFELD-MÜHLENHÖHE STATION 13

3. THE INFLUENCE OF SYNOPTIC ATMOSPHERIC PRESSURE FLUCTUATIONS ON TILT MEASUREMENTS 15

3.1 Previous Studies 15
3.2 Empirical Relationship between Local Air Pressure Fluctuations and Tilt 17
3.3 Model Calculations for Evaluating the Influence of Air Pressure on Tilt Measurements 20
3.3.1 Methods of Analysis 21
3.3.1.1 Analytical Solutions of the Boussinesq Problem 21
3.3.1.2 The Finite Element Method 23
3.3.2 Evaluation of the Magnitude of Deformation 24
3.3.2.1 Comparison of the Vertical Displacements Calculated for a Plane Model and a Spherical Model 24
3.3.2.2 Analytical Evaluation of the Amount of Deformation for a Load Imposed by a High Pressure System 26
3.3.2.3 Comparison of Horizontal and Vertical Tilts with the Use of the Finite Element Method 28
3.3.2.4 Depth Dependence of Tilt for Surface Loads 29
3.3.3 Evaluation of the Attraction Effect 31
3.3.4 Summary of Results 32

4. THE INFLUENCE OF LOCAL PRECIPITATION ON TILT MEASUREMENTS 33

4.1 Empirical Correlation between the Amount of Precipitation and Tilt 33

4.2 Quantitative Investigations 37
4.2.1 Experimental Prerequisities 37
4.2.2 Prediction of the Tilt Signal by the Amount of Precipitation per Unit Time 38
4.2.3 Influence of the Precipitation Signal on the Analysis of the Tides 41
4.3 Discussion of Different Model Concepts 41
4.3.1 Heat Transfer through Precipitation 42
4.3.2 Expansion Effects from Clay Minerals 44
4.3.3 Load Effects from Precipitation 45
4.3.4 Lateral Fluctuations of the Fracture Water Level 46
4.3.4.1 Geological Description of the Fracture System 46
4.3.4.2 Model of the Fracture System and Results of Tilt Calculations 46
4.3.4.3 Possible Causes of the Lateral Differences in the Fracture System Water Level 49
4.3.4.4 Compatibility of the Model with the Preferred Direction of Tilt 52
4.3.4.5 Evaluation of the Model 52
4.3.5 Geological Disturbances in the Area of the Station 53
4.4 Results and Consequences 56

5. SECULAR TILTS 57

5.1 Annual Fluctuations in the Ground Temperature and Long-Period Tilts 59
5.1.1 Preliminary Evaluation in the Time Domain 59
5.1.2 Spectral Analysis of Tilt and Temperature Data with the Maximum Entropy Method 60
5.1.2.1 Characteristics of the Maximum Entropy Method (MEM) 60
5.1.2.2 Spectral Analysis and its Results 62
5.1.3 Amplitude and Phase Determinations 67
5.1.4 Model Considerations 68
5.1.5 Model Calculations of Thermoelastic Distortions in the Bedrock with the Finite Element Method 69
5.1.5.1 The Topographic Model of the Zellerfeld-Mühlenhöhe Station 69
5.1.5.2 Discussion of the Results of the Model Calculations 72
5.1.5.3 Sensitivity of the Results to Variations of the Model Parameters 74
5.2 Other Effects with an Annual Periodicity 75
5.3 Aperiodic Portions of the Signal 77
5.3.1 Composition of the Long-Term Drift 77
5.3.2 Possible Origin of the Aperiodic Components 80

6. SUMMARY 81

REFERENCES 85

BIOGRAPHY 89

Illustrations

2.1. Site Plan of Zellerfeld-Mühlenhöhe Station 15

3.1. Surface Pressure Distribution over Central Europe (air pressure in mb), a. 6 February 1974, 0100 hours, b. 7 February 1974, 0100 hours 18

3.2. Comparison of the Recordings of the Two Tiltmeters P1 and P3 with the Curve of the Air Pressure at the Clausthal-Zellerfeld Weather Station During the So-Called Hundred-Year Minimum (installation depth: P1 = 30 m; P3 = 15 m) 19

3.3. Illustration of the Different Correlations Between Air Pressure Variations and Tilt Variations by Comparison of Recordings of the Tiltmeters with the Local Air Pressure Curve (installation depth: P1 = 30 m; P3 = 15 m) 20

3.4. Comparison of the Vertical Displacements u on the Earth's Surface for Different Loading Models, that is, for z = 0 (——— = discoid load on Bullen's earth model; -.-.- = discoid and ----- = elliptical loads on a homogeneous plane half-space) 25

3.5. Model of the Load Δp with an Elliptical Cross-Section Acting on an Infinitely Extended, Plane, Homogeneous, Isotropic, Elastic Half-Space (λ, μ = Lamé constants; α = radius of the loaded surface) 26

3.6. The Tilt Change ΔN Resulting from the Deformation Under a Load (see Figure 3.5) as a Function of the Distance r from the Center of the Load, Calculated According to Equation (3.8) (curve parameters: radius α of the load) 27

3.7. Comparison of the Horizontal Tilts Calculated According to the Boussinesq Method (-o-o-) and the Finite Element Method (-x-x-) with the Vertical Tilt Changes Calculated by Means of the FEM for a Discoid Load 29

3.8. Lines of Equal Vertical Tilt, Given in 10^{-3}", for Loading on a Homogeneous, Plane Half-Space (parameters as in Figure 3.6) 30

3.9. Attraction-Caused Tilts ΔN Due to a Changed Density Distribution in the Atmosphere as a Function of the Distance r from the Center of the Load with the Radius α of the Loaded Surface as a Parameter 32

4.1. Connection Between the Tilt Change Due to Air Temperature T and Precipitation Ns (given with respect to the time interval between the meteorological recording times 0700, 1400, 2100; precipitation and temperature data: Clausthal-Zellerfeld Weather Station) 34

4.2. Influence of Precipitation (symbols as in Figure 4.1) and Melting Phase (Tw) on Tilt; Comparison of the Local Air Pressure Variation with the Amount of Precipitation per Day (installation of depth: P1 = 30 m; P3 = 15 m) 35

4.3. Example of the Behavior of the Tilt ΔN over Time (x component of P1, installation depth 30 m) with the Appearance of Rainfall 36

4.4. Description of the Connection Between Amount of Precipitation and Tilt Change by Means of a Linear System 38

4.5. Result of the Prediction of the Tilt Signal ΔN with the Use of the Parameter: Amount of Precipitation per Hour Ns (mm/h) 40

4.6. Thermoelastically Caused Tilt Changes at ΔN for Temperature Changes ΔT in the Region of the Damming Layer 43

4.7. Model of a Beam Stressed on One Side 47

4.8. Tilt Change ΔN as a Function of the Thickness b of the Rock Plate with Effective Force ($-\Delta p \cdot \Delta z$) as a Parameter (corresponding water level changes: from the bottom 6, 12, 24, 48, 96 mm) 48

4.9. Model for the Qualitative Description of the Pressure and, Therefore, Tilt Behavior with Different Permeabilities k_1, k_2 in the Surficial Layer, (a) With a Horizontal Surface, (b) With an Inclined Surface and Surface Runoff ($\Delta(\Delta p)$ = differential pressure between 1 and 2) 50

4.10. Model with Different Thicknesses of the Weathered Layer for a Qualitative Explanation of the Pressure Behavior and the Resulting Tilt Variation, (a) Without Surface Runoff, (b) With Surface Runoff, ($\Delta(\Delta p)$ = differential pressure between 1 and 2) 51

4.11. Sketch of the Model Used for the Finite Element Calculations B1 = block length; Bh = block height; E = modulus of elasticity; σ = Poisson's ratio; F = applied force) 53

4.12. Tilt Changes at Depths of 15 m (ΔN_{15}) and 30 m (ΔN_{30}) and Their Ratio as a Function of the Depth in Which a Pressure Change $\Delta p = 0.981 \cdot 10^5$ dyn/cm^2 ($\hat{=}$ 1 m of water is present) 54

4.13. Tilt Changes at Depths of 15 m (ΔN_{15}) and 30 m (ΔN_{30}) and Their Ratio as a Function of the Block Length (block height = 50 m; pressure change $\hat{=}$ 2 m of water) 55

4.14. Tilt Changes at a Depth of 15 m (ΔN_{15}) and 30 m (ΔN_{30}) and Their Ratio as a Function of the Distance from the Left Edge of the Block (block height = 50 m; $\Delta p \hat{=}$ 2 m of water) 56

5.1. Comparison of Long-Period Tilt Components with the Annual Variation of the Ground Temperature 60

5.2. Tilt Changes in the Period Range over 120 Days for the EW and NS Components of P1 (installation depth 30 m) and P3 (installation depth 15 m); --- Linear Drift Component (according to Flach et al[19]) 63

5.3. ME-Spectra of the Tilts from the Four Tiltmeter Components in the Period Range over 120 Days and of the Ground Temperature Measured at a Depth of 1 m (-o-o = ground temperature; ---- = EW-P1; —— = NS-P1; ..... = EW-P3; -.-.- = NS-P3) 65

5.4. ME-Spectra of the Tilts from the Four Tiltmeter Components After Drift Elimination and of the Ground Temperature at a Depth of 1 m 66

5.5. Two Dimensional Finite Element Model of the Zellerfeld-Mühlenhöhe Station (EW direction) 70

5.6. Approximation of the Temperature Distribution with Depth with the Use of the Temperature-Depth Functions Calculated at Ten-Day Intervals (—— = calculated temperature-depth functions (thermal conductivity 10^{-2} cm^2/sec), · = nodal point temperatures between which temperatures are linearly interpolated) 71

5.7. Cross-Section with Lines of Equal (Maximum) Tilt Changes (in 10^{-3}") Which Result from the Annual Variation of the Ground Temperature 72

5.8. Vertical Tilt Variations ΔN in the Case of Loading from Water Level Fluctuations in Stadtweger Pond as a Function of the Distance r (model of a homogeneous plane halfspace) 76

5.9. Comparison of the Annual Tilt Variations of YP3 with the Water Level Fluctuations in Stadtweger Pond 76

5.10. Aperiodic Portions of the Drift in the Case of Approximation with a Parabola of the Second Order for P1 and P3 (installation depths: P1 = 30 m; P3 = 15 m) 78

5.11. Survey of the Most Important Veins and Ranges of Veins in the Northwestern Oberharz (according to Hinze[23]) 79

5.12. Comparison of the Long and Aperiodic Tilt Components Separated by Numerical Filtering (——) with the Component Calculated by Summation of the Steps (-. -.) as well as its Linear Portion (-----) During the Period 20 January 1974 to 20 July 1975 for the X-Component of P1 80

Tables

2.1. Setup of Boreholes and Tiltmeters 14

3.1. Geometry and Elastic Parameters of Bullen's Earth Model (R_1, R_2 = internal-external radii; λ, μ = Lamé constants; σ = Poisson's ratio) 24

5.1. Length of the Analysis Intervals and the Prediction-Error-Operators 65

5.2. Length of the Analysis Intervals and of the Prediction Error-Operators After Drift Removal (see Figure 5.4) 66

5.3. Results of the Amplitude and Phase Calculations 67

5.4. Summary of the Model Parameters 71

Interpretation of Tilt Measurements in the Period Range Above That of the Tides

1. INTRODUCTION

For several decades measurements of tilt, strain, and gravity variations, caused by the earth's body tides, have been carried out for the purpose of determining the internal elastic properties of the earth. This task represents the classical problem of research into the earth's body tides; its solution appeared to have very good prospects for rapid success, in particular because of the fact that the tide generating forces are known with great accuracy. The result of studies performed up to now, represented by a large number of publications with the results of analyses of tiltmeter and gravimeter measurements, however, reveal significant problems. Thus, for example, the semi-diurnal lunar tide M_2, which is the tidal component least disturbed by nontidal influences, displays deviations from the theoretically expected tilts (anomalies) of ±40 percent in the North-South direction and ±15 percent in the East-West direction; the anomalies in the gravity variations are 8 percent without correction for load effects from ocean tides. The phases determined from tilt measurements display fluctuations of a maximum of $\pm 10^{\circ}$, while those determined from gravimeter data display fluctuations of $\pm 2^{\circ}$ (Lennon and Baker[1]).

(Received for publication 23 April 1979)

1. Lennon, G. W. and Baker, T. F. (1973) Earth tides and their place in geophysics, Phil. Trans. R. Soc., London A274:199-202.

The accuracy of tiltmeters and gravimeters has become so high in recent years that the anomalies measured cannot be attributed to the instruments. Thus, today, with the specifications which set the limit of accuracy on the instruments, reproducibilities of ±1 percent (Bachem,[2] Bonatz and Rocholl[3]), are obtained with horizontal pendulums, and even of ±0.2 percent with Askania borehole tiltmeters (Grosse-Brauckmann[4]) and with gravimeters (Wenzel[5]).

Therefore, it is necessary to deal with the problem of the installation of the instruments as well as the problem of the influence of the observation point, especially on tilt and strain measurements. The numerical treatment of these problems by Harrison[6, 7] shows that underground cavities in which strain and tilt measuring instruments usually are installed are greatly deformed under the influence of tidal strain. Therefore, the strain measured in the area of the cavity usually does not agree with that in the surrounding bedrock, and there are local strain-induced tilts which, in particular for instruments with a short base, lead to large errors in the results. This cavity effect is avoided by the installation of the tiltmeters in boreholes. In addition, such strain-induced tilts are also caused by the topography of the area around the station, by the surrounding geological structures, as well as by inhomogeneities in the elastic properties of the bedrock. Moreover, the measurements are influenced by a perturbing effect with the same periods as the earth's body tides, namely by the load effect of the oceanic tides (Farrell[8]). In the case of strain measurements, the deviations between observed and theoretical tides can be largely eliminated by the application of appropriate corrections (Levine and Harrison,[9] Berger and Beaumont[10]). On the other hand, the use of corrections for tilt measurements does not lead to this goal, as the measurements with tiltmeters with very short bases are contaminated by local strain-induced tilts. These tilts are caused by inhomogeneities at the point of installation and fractures and cracks in the bedrock, which cannot be modelled.

Until now, the effects discussed have been studied exclusively with respect to their effect on tidal tilt and strain. The idea and the first analytical calculations go back to King and Bilham.[11] On the other hand, attempts to attribute the differences between measured and expected tides on factors which are effective predominantly in the period range greater than that of the tides, but which also exhibit some signal in the tidal range, are considerably older. This is essentially a matter of meteorolcgical influences such as air pressure and temperature fluctuations as well as precipitation effects. The first studied were by Lettau[12, 13] and Tomaschek.[14] Later, Simon,[15] Tanaka,[16] Herbst,[17] and Zschau,[18] among others, attempted to solve this problem exclusively with statistical methods.

Due to the number of references to be included as footnotes on this page, the reader is referred to the list of references, page 85.

These studies show that there are significant correlations between the meteorological factors considered and the tilt, and that the use of the appropriate corrections to the tides also leads to an improvement in the results. The synthesis of the statistical results into physically plausible models, however, has not been achieved satisfactorily as yet. This goal appears to be unattainable without supplementary model calculations.

The meteorological effects, however, are interesting not only because of their influence on the tides. Apart from the fact that it is fundamentally desirable to know the informational content from a group of measurements as completely as possible, it is necessary to determine how these effects can be used to deal with further geodynamic problems. In addition, such investigations can provide important information about the most efficient choice of the observation point and type of installation of tiltmeters so that the signal-to-noise ratio can be favorably enhanced with respect to the phenomena of primary interest. These considerations are particularly interesting in connection with the investigation of recent crustal movements such as those occurring in tectonically active regions, for example, as precursory phenomena in the case of earthquakes. The degree of accuracy to which all the influences due to these aperiodic effects can be eliminated determines the usefulness of the research methods used.

The present study should provide a contribution to the interpretation of tilt measurements, and thus contribute to the clarification of the problems involved. For this purpose, the data from two Askania borehole tiltmeters at the Zellerfeld-Mühlenhöhe Station, operating at tidal periods, are analyzed with statistical and deterministic methods. In particular, the influences of atmospheric pressure fluctuations, precipitation, and subsurface temperature fluctuations are investigated for the purpose of obtaining the most complete interpretation of the tilt measurements possible. Models are developed for the individual effects. The models are evaluated, insofar as possible, by analytical methods; problems which are not solvable analytically, are analyzed with the finite element method. The treatment of the problems and the presentation of results is carried out in such a fashion that the signals with periods of several days are investigated first, and then the long and aperiodic portions of the signals.

2. DESCRIPTION OF THE ZELLERFELD-MÜHLENHÖHE STATION

Since 1969, tilt measurements have been carried out at the Zellerfeld-Mühlenhöhe Station with Askania borehole tiltmeters. The long-term recordings serve the purpose of solving a number of instrumental and technique evaluation problems as well as providing data for the investigation of geodynamic problems

(Flach, Grosse-Brauckmann, Herbst, Jentzsch, and Rosenbach).[19] The reader is referred to the publications by Flach and Rosenbach[20] and Flach, Rosenbach and Wilhelm[21] for the technical details of the tiltmeter installation, as well as a detailed description of the station.

The information necessary for this study is summarized briefly below.

The Zellerfeld-Mühlenhöhe Station lies on the north edge of the Zellerfeld district (see Figure 2.1), at an altitude of 585 meters. It has the geographical coordinates $\phi_N = 51^{\circ}49'20''$ and $\lambda_E = 10^{\circ}20'30''$. Table 2.1 gives information on the depth of the boreholes, the tiltmeters in them, and their orientation.

Table 2.1. Setup of Boreholes and Tiltmeters

Tiltmeter	Depth of Borehole	Components	Azimuth toward N
P1	30 m	X (KA1)	$303^{\circ}16'$
		Y (KA2)	$33^{\circ}16'$
P3	15 m	X (KA5)	$125^{\circ}21'$
		Y (KA6)	$215^{\circ}21'$

The boreholes were sunk approximately 15 meters apart in Upper Harz Culm graywackes, which have inclusions of graywacke slate and clay slate. A description of the tectonic elements, which characterize the Clausthaler Culm fault zone, is given by Mohr[22] and Hinze[23] (see also Sections 4.3.4.1 and 5.3.1). The local geological relationships allow a subdivision into three layers, which is based on a geological interpretation of the boreholes by the Institute of Geology of the

19. Flach, D., Grosse-Brauckmann, W., Herbst, K., Jentzsch, G., and Rosenbach, O. (1975) Results of long-term recordings with Askania borehole tiltmeters – Comparative analysis with respect to the tide parameters and long-period portions and instrumental investigations, Deutsche Geodät. Komm. B211:72-95.

20. Flach, D. and Rosenbach, O. (1971) The Askania borehole tiltmeter (tide pendulum) of A. Graf at the Zellerfeld-Mühlenhöhe testing station, Bull. Inf. Mar. Terr. 60:2934-2943.

21. Flach, D., Rosenbach, O., and Wilhelm, H. (1971) Investigations of A. Graf's Askania borehole tiltmeter (tide pendulum) at the Zellerfeld-Mühlenhöhe testing station, Bull. Inf. Mar. Terr. 60:2944-2954.

22. Mohr, K. (1973) Western Part of the Harz – A Collection of Geological Guides 58, Borntraeger, Berline-Stuttgart.

23. Hinze, C. (1971) Legend for Clausthal-Zellerfeld Paper No. 4128 (Geological Map of Niedersachsen 1:25,000), Nieder Sachsen Office for Geological Research, Hannover.

Clausthal Technical University. The unconsolidated layer has a thickness of between 0 and 2 meters; it is underlain by a layer of weathered graywacke between 6 and 8 meters thick, and then from about 8 to 10 meters, by a consolidated graywacke (see Table 5.4).

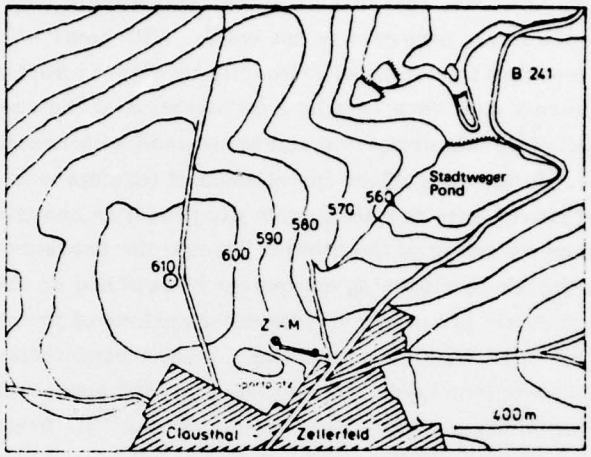


Figure 2.1. Site Plan of Zellerfeld-Mühlenhöhe Station

3. THE INFLUENCE OF SYNOPTIC ATMOSPHERIC PRESSURE FLUCTUATIONS ON TILT MEASUREMENTS

3.1 Previous Studies

Significant impetus for the investigation of the influence of barometric load changes on tilt and gravimetric measurements came from Tomaschek.[14] From a seven-day recording of the deflection of the vertical, he drew the conclusion that there is a correlation between the barometric pressure distribution over a region extending from Greenland to the European continent and the tilts and vertical displacements observed in Winsford in the British Isles. He interprets the movements which appear as tilts of greatly extended plates, more or less movable as a block, the tilt axis of which may be assumed to be at least 300 km northwest of the measuring station. Because of the short observation period, this interpretation, however, must be treated with caution. Zschau[18] has suggested that the effects measured possibly may be attributed to water level fluctuations in the Irish Sea caused by air pressure.

Also, Simon[15] and Simon and Schneider,[24] on the basis of statistical investigations of long-term tilt measurements which they are conducting, find a significant correlation between tilts in the period range of several days and fluctuations of local air pressure. The tilts which appear are, as in the case of Tomaschek,[14] interpreted as large area block tilts under the influence of barometric load changes. Later studies show, however, that this comparatively simple representation of the complicated influence of air pressure is not valid. With some of the tiltmeters used, the effects measured are caused primarily by direct effect of air pressure on the instruments and, thus, not by a deformation of the earth's surface (Simon and Schneider[25]); this distortion can be avoided with pressure-tight sealing of the instruments. In the case of the installation of tiltmeters in underground chambers, ground movements resulting from air pressure changes may appear as a result of the air conditioning of the mine workings; the pressure fluctuations which occur when the air conditioning equipment is switched on and off, as compared with the surface air pressure, create deformations of the measuring chamber which couple into a tilting of the mountings of the instruments. In addition, deformations of a subsurface layer from a changing load appear as the result of changes in the regional air pressure distribution (Simon[26]). In the case of this effect it may be assumed that it is greatly distorted because measurements are made in underground cavities lying in geologically disturbed zones; in other words, the deformations measured in the chambers are not identical with those of the surrounding bedrock.

The disadvantages connected with the installation of tiltmeters in underground measuring chambers (cavity and geological effects), are avoided by emplacement of the instruments in boreholes. The Askania borehole tiltmeter is intended for such an installation. In addition, the influence of small scale inhomogeneities and discontinuities in the bedrock is reduced by the ten times greater base length as compared with that of horizontal pendulums. Investigations of the influence of meteorological effects on data obtained with these tiltmeters were conducted by Zschau[18] for the Kiel-Rehmsberg Station and by Herbst[17] for the Zellerfeld-Mühlenhöhe Station. In both cases a significant correlation between

---

24. Simon, D. and Schneider, M. (1967) The appearance of air pressure-induced distortions in horizontal pendulum readings at three different earth tide stations, Bull. Inf. Mar. Terr. 49:2218-2225.

25. Simon, D. and Schneider, M. (1973) Analysis of the nonperiodic ground deformations at the Tiefenort Tidal Station 1958-1973, Geodät. Geophys. Veröff. Series III.

26. Simon, D. (1975) Coherence of Tidal Parameters Observed at Tiefenort (GDR) with Respect to Pseudo-Tidal Effects Induced by Atmospheric Pressure Variations, Report presented to the XVI General Meeting of the IUGG, Grenoble.

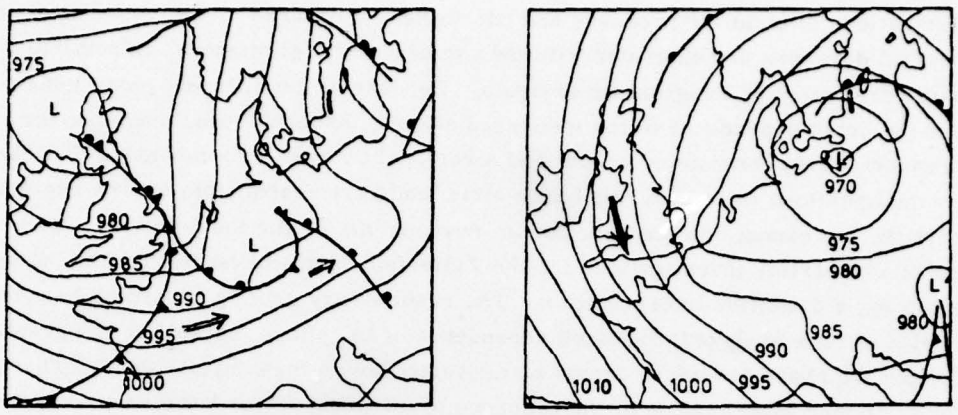
fluctuations of local air pressure and tilt changes measured in the period range of several days was demonstrated with the use of statistical methods, in particular with correlation and regression analysis. Because of the different phase behavior and the depth dependence of the measured effects, Zschau[18] concludes that the air pressure effect consists of a local and a regional portion. He considers that elastic deformations from changing barometric loads are responsible for the regional portion, but cannot cite any mechanism responsible for the local portion. The results of earlier investigations for the Zellerfeld-Mühlenhöhe Station also do not allow for a definitive interpretation. The results vary greatly according to the period of time analyzed; the depth dependence of the effect, as well as the greatly fluctuating phase behavior, cannot be converted into a meaningful model. Therefore, further investigation of the influence of air pressure on tilt measurements is necessary.

3.2 Empirical Relationship between Local Air Pressure Fluctuations and Tilt

The use of statistical methods for identifying any cause-and-effect among the measured variables presupposes stationarity of the time series being compared. However, in general, the time series do not possess this property, for example, because of aperiodic drifts. Therefore, stationarity is created with the use of appropriate numerical filters. In this way, specific portions of the signal are suppressed according to the filter properties. The information which is contained in the unfiltered series, therefore, is reduced and the form of the signals is changed. In order to counter the problems connected with this (see Section 4.1), we proceed without the numerical filtering and conduct the investigations on untreated data.

Next, the effect of an extreme air pressure variation, that of the so-called hundred-year minimum (1974), is examined in order to test current theories on the influence of air pressure. The weather conditions were as follows: on 5 February 1974 an extensive cyclonic low formed over Scotland, the center of which moved over northwest Germany during 6-7 February (see Figure 3.1), and moved slowly to the east while weakening. These weather conditions differed from the typical conditions for northern Germany in that here, instead of the edges of low pressure cells moving over northern Germany while the centers passed over the British Isles, the center of the cyclonic low itself moved over northern Germany. This was documented by the fact that the air pressure dropped to values of 40 mb below normal. A minimum of 898.9 mb was measured at the Braunlage Weather Station (see Figure 3.2).

According to current concepts, an obvious disturbance in the tilt recordings should have appeared near the time of the large pressure drop. However, the two components of both tiltmeters showed no effect during the period from



(a) 6 February 1974, 0100 hours (b) 7 February 1974, 0100 hours

Figure 3.1. Surface Pressure Distribution over Central Europe (air pressure in mb)

5 February to 8 February. A rapid excursion in both components first began on 9 February, and the maximum deviation in the EW components was about $180 \cdot 10^{-3}$" for P3, and about $100 \cdot 10^{-3}$" for P1. The phase difference relative to the air pressure of 4 to 5 days is much too great for a meaningful matching of the air pressure signal and the tilt signal to be possible. In addition, a consideration of the amplitudes shows a distinct depth dependence of the disturbance, the observed effects being only about half as great at a depth of 30 m as at a depth of 15 m. If the model of large scale elastic deformations is based on barometric load changes, this reduction of the tilt effect with depth cannot be explained, since a variation of 15 meters in the measuring depth should create no significant change in the tilt signal (see Section 3.3.2.4).

The example cited may be viewed as characteristic of many others. Figure 3.3 shows that the corresponding conclusions also may be drawn from recordings made over longer periods. Although occasionally tilt changes coincide with the larger air pressure fluctuations, there are also examples where air pressure fluctuations of the same order of magnitude lead to no disturbance in the tilt recordings. In particular, the extreme tilt changes in the months of February and March 1973 cannot be explained by air pressure fluctuations. The reasons for the occasionally existing correlation between these values are explored in greater detail in Section 4.1.

These simple considerations show that even extreme air pressure fluctuations are not capable of directly creating tilt effects of the order of magnitude postulated, for example, by Tomaschek, [14] Simon, [15] and Zschau, [18] that is, a multiple of the

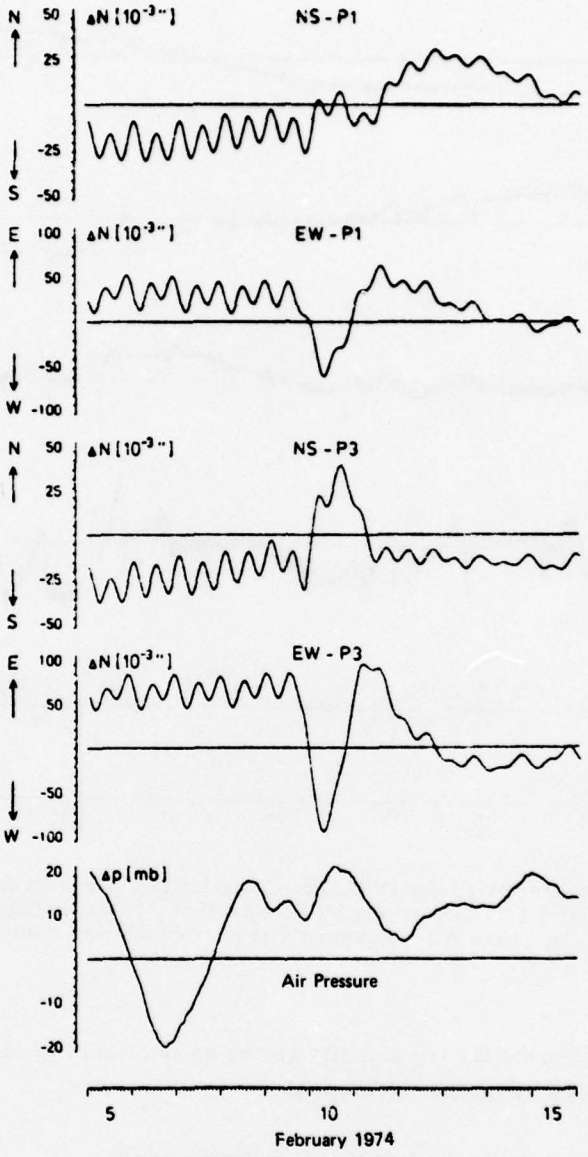


Figure 3.2. Comparison of the Recordings of the Two Tiltmeters P1 and P3 with the Curve of the Air Pressure at the Clausthal-Zellerfeld Weather Station During the So-Called Hundred-Year Minimum (installation depth: P1 = 30 m; P3 = 15 m)

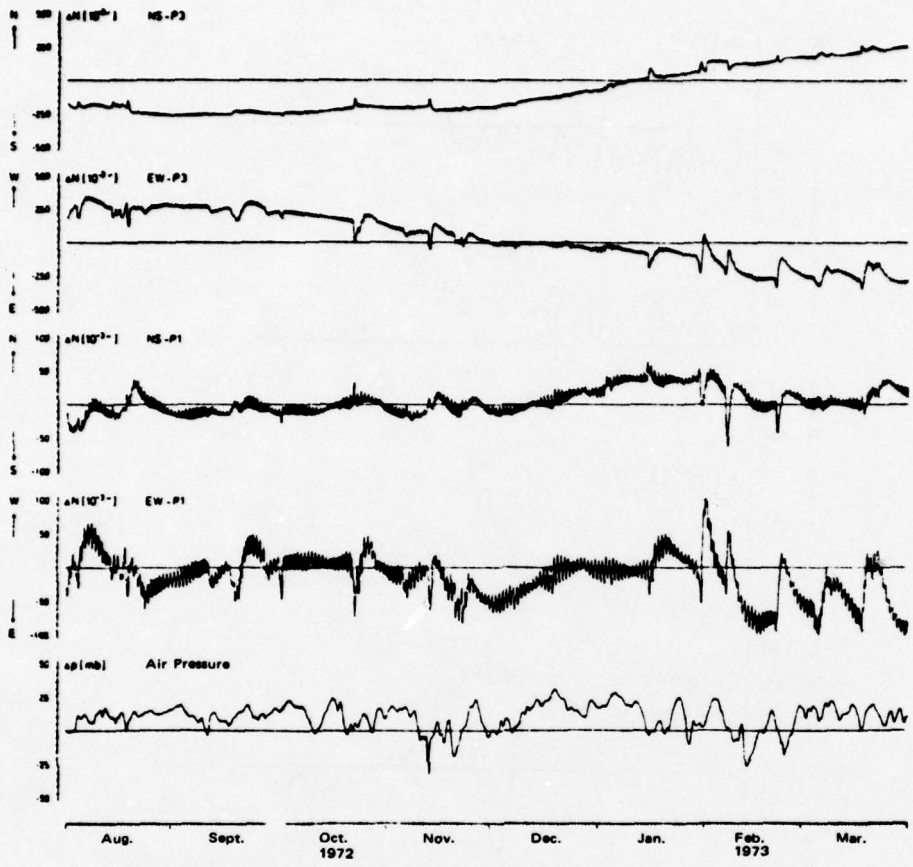


Figure 3.3. Illustration of the Different Correlations Between Air Pressure Variations and Tilt Variations by Comparison of Recordings of the Tiltmeters with the Local Air Pressure Curve (installation depth: P1 = 30 m; P3 = 15 m)

tidal amplitude. How great the tilt actually varies as the result of elastic deformations must be explained by model calculations.

3.3 Model Calculations for Evaluating the Influence of Air Pressure on Tilt Measurements

Variations in the air pressure distribution may affect tilt measurements in three ways:

1) by the deformation of the earth's surface because of the changing load of the air masses;

2) by the gravitational effect by the changing air mass distribution over the area under consideration; it creates a direct attraction force, in this specific case, on the pendulum mass of the Askania borehole tiltmeter;

3) by the variation of the gravity potential because of the altered mass distribution of the deformed earth; this portion is small in relation to the gravitational effect and, therefore, may be ignored.

3.3.1 METHODS OF ANALYSIS

3.3.1.1 Analytical Solutions of the Boussinesq Problem

The calculation of the static deformation of a nongravitating homogeneous elastic half-space under the influence of surface pressure, goes back to Boussinesq.[27] The static displacement vector $\vec{s}$, satisfies the differential equation of elastic equilibrium

$$(\lambda + 2\mu)\nabla\nabla \cdot \vec{s} - \mu\nabla \times \nabla \times \vec{s} = 0 \tag{3.1}$$

where λ and μ are the Lamé constants.

In a cylindrical coordinate system with the unit vectors $\vec{e}_z$, $\vec{e}_r$, and $\vec{e}_\theta$ the volume which fills the half-space is described by $z < 0$. Solutions of Equation (3.1) are sought under the condition that the free surface for a point load is originally unstressed. Because of the axial symmetry of the load, the solution is independent of θ, and the displacement vector $\vec{s}$, is completely described by

$$\vec{s} = u(z, r)\,\vec{e}_z + v(z, r)\,\vec{e}_r \tag{3.2}$$

where u is the vertical component and v the horizontal.

The standard solution for the displacements which are created by a unit point force applied perpendicular to the surface is provided by Farrell[8]

$$u(z, r) = -\frac{1}{4\pi\mu R}\left(\frac{\sigma}{\eta} + \frac{z^2}{R^2}\right)$$

$$v(z, r) = -\frac{1}{4\pi\eta r}\left(1 + \frac{z}{R} + \frac{\eta r^2 z}{\mu R^3}\right) \tag{3.3}$$

with $\eta = \lambda + \mu$ and $R^2 = r^2 + z^2$.

---

27. Boussinesq, J. (1885) Application of the Potential to the Study of the Equilibrium and the Movement of Elastic Solids, Gauthier-Villars, Paris.

Discoid and elliptical loads are better suited to the problems to be analyzed than is a point load. Of course, these types of loads permit a formal calculation of the displacement vectors only on the surface of the half-space, that is, for $z = 0$ (see Equations (3.4) to (3.7)). Therefore, only the horizontal tilt changes can be calculated, and not, as would be necessary with the use of an instrument with a vertical baseline, the vertical tilt changes. Section 3.3.2.3 deals with the problem of to what extent the calculated horizontal tilts are useful for evaluating the maximum tilt effects which appear in spite of this limitation.

The solution for a discoid load with radius α is (Farrell[8])

$$u(0, r) = -\frac{\sigma}{\pi^2 \mu \eta \alpha} E\left(\frac{r}{\alpha}\right) \qquad r < \alpha$$

$$u(0, r) = -\frac{\sigma r}{\pi^2 \mu \eta \alpha^2}\left[E\left(\frac{\alpha}{r}\right) - \left(1 - \frac{\alpha^2}{r^2}\right) K\left(\frac{\alpha}{r}\right)\right] \qquad r > \alpha \tag{3.4}$$

and

$$v(0, r) = -\frac{r}{4 \pi \eta \alpha^2} \qquad r < \alpha$$

$$v(0, r) = -\frac{1}{4 \pi \eta r} \qquad r > \alpha \tag{3.5}$$

with the complete elliptical integrals of the first and second kinds

$$E(k) = \int_0^{\pi/2} (1 - k^2 \sin^2 \phi)^{1/2} \, d\phi$$

$$K(k) = \int_0^{\pi/2} (1 - k^2 \sin^2 \phi)^{-1/2} \, d\phi \quad .$$

Compared with a discoid load, an elliptical load has the advantage that the pressure gradually approaches zero near the edge. This model represents a better approximation, in particular for loads resulting from air pressure. The appropriate components of the displacement vector are calculated according to (Farrell[8])

$$u(0, r) = -\frac{3\sigma}{16\,\mu\,\eta\,\alpha}\left(1 - \frac{r^2}{2\alpha^2}\right) \qquad r < \alpha$$

$$u(0, r) = -\frac{3\sigma}{8\,\pi\,\mu\,\eta\,\alpha}\left[\left(1 - \frac{r^2}{2\alpha^2}\right)\sin^{-1}\left(\frac{\alpha}{r}\right) + \frac{r}{2\alpha}\left(1 - \frac{\alpha^2}{r^2}\right)^{1/2}\right] \qquad r > \alpha \tag{3.6}$$

and

$$v(0, r) = -\frac{1}{4\,\pi\,\eta\,r}\left[\left(1 - \left(1 - \frac{r^2}{\alpha^2}\right)^{3/2}\right]\right. \qquad r < \alpha$$

$$v(0, r) = -\frac{1}{4\,\pi\,\eta\,r} \qquad r > \alpha \quad . \tag{3.7}$$

3.3.1.2 The Finite Element Method

The finite element method is a numerical technique which is particularly suitable when the analytical solution of a physical problem is no longer possible, or possible only for very limited conditions. The method is based on the assumption that the continuum with an infinite number of connection points can be replaced by discrete elements into which individual groups of points are combined and which are interconnected at a finite number of points. This results in the formation of a finite system of albegraic equations which are exactly solvable. With the use of the so-called "equilibrium" statement, according to the variational principle, we have a system of symmetrical linear equations

$$[K]\{\delta\} - \{R\} = 0$$

where $\{R\}$ includes the body forces; the coupling with the unknown displacements $\{\delta\}$ takes place through the matrix $\{K\}$, which includes information on the type of element approximation and the linear mechanical properties of the continuum.

This method has already been used for some time in the engineering sciences; Zienkiewicz,[28] for example, presents a detailed description of the fundamentals and examples of application. In recent years, the method has found use in geophysics,

---

28. Zienkiewicz, O.C. (1971) The Finite Element Method in Engineering Science, McGraw-Hill, London.

for example in the area of tilt measurements (Beaumont and Lambert,[29] and Harrison[6, 7]).

The computer program SAP IV is used for model calculations for the static and dynamic analysis of linear systems (Bathe, Wilson, and Peterson[30]). It was available for use on the computer of the Niedersachsen Computer Center in Hannover in February 1976.

3.3.2 EVALUATION OF THE MAGNITUDE OF DEFORMATION

3.3.2.1 Comparison of the Vertical Displacements Calculated for a Plane Model and a Spherical Model

In order to determine whether the simple model of a plane, homogeneous, elastic half-space suffices for the proposed evaluation of the influence of air pressure, the Boussinesq calculations for a plane model are compared with calculations which were performed by Slichter and Caputo[31] for a modified spherical model of the earth (Bullen[32]). In this way, it is possible on the one hand to verify the correctness of the numerical calculations, and on the other, to evaluate the influence of the model on the results. The geometric and the elastic parameters for Bullen's earth model are tabulated in Table 3.1.

Table 3.1. Geometry and Elastic Parameters of Bullen's Earth Model (R_1, R_2 = internal-external radii; λ, μ = Lamé constants; σ = Poisson's ratio)

	R_1, R_2 [km]	λ [dyn/cm^2]	μ [dyn/cm^2]	σ
Crust	6371 - 3472	$1.273 \cdot 10^{12}$	10^{12}	0.28
Core	3472 - 0	$8 \cdot 10^{12}$	0	0.5

---

29. Beaumont, C. and Lambert, A. (1972) Crustal structure from surface load tilts, using a finite element model, Geophys. J. Roy. Astrom. Soc. 29:203-206.

30. Bathe, K.-J., Wilson, E.L., and Peterson, F.E. (1973) SAP IV – A Structural Analysis Program of Static and Dynamic Response of Linear Systems, Report No. EERS 73-11, Earthquake Engineering Research Center, University of California, Berkeley.

31. Slichter, L.B., and Caputo, M. (1960) Deformation of an earth model by surface pressures, J. Geophys. Res. 65:4151-4156.

32. Bullen, K.E. (1947) An Introduction to the Theory of Seismology, Cambridge Univ. Press.

The model is stressed with a circular load (the pressure is constant over the entire loaded surface), and the components of the displacement vector are calculated as a function of the distance on the earth's surface. The vertical displacements for the spherical model given by Slichter and Caputo are presented in Figure 3.4.

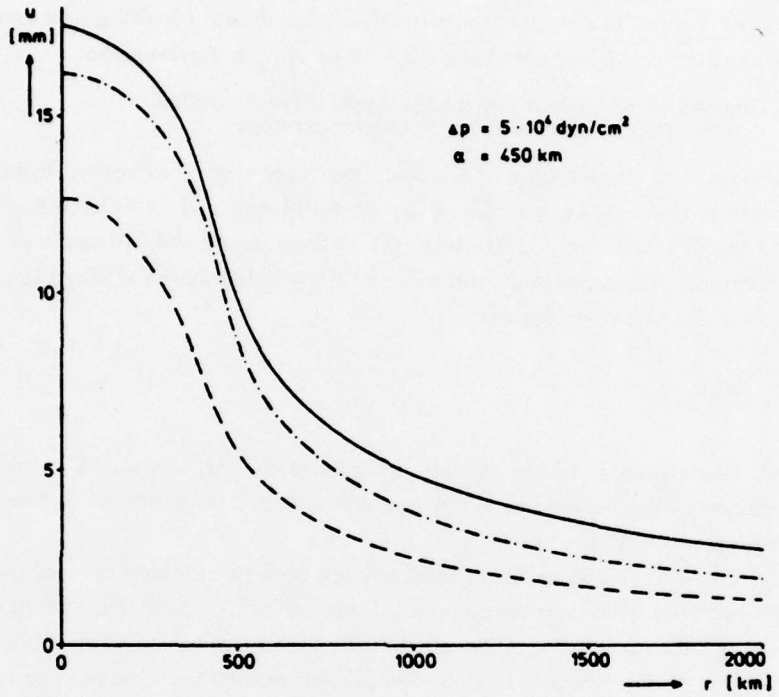


Figure 3.4. Comparison of the Vertical Displacements u on the Earth's Surface for Different Loading Models, that is, for z = 0 (——— = discoid load on Bullen's earth model; - · - · - = discoid and ----- = elliptical loads on a homogeneous plane half-space)

The z-displacements for the plane, homogeneous, elastic half-space according to Equation (3.5) are given for comparison. The elastic parameters are identical with those of the outer crust of the spherical model; in both cases the pressure is $5 \cdot 10^4$ dyn/cm^2 and the radius of the loaded surface is 450 km. The difference of the displacements in the z-direction is always smaller than 1 mm; in particular, in the region outside of the loaded surface the two curves are almost parallel, that is, the resulting tilts barely differ. The two models can be viewed as equivalent for the maximum 2000 km distances to the center of the load considered for the

calculation. This fact indicates that consideration of the elastic properties to a depth which is of the order of magnitude of the distance from the center of the load to the observation point is sufficient for determining the displacements with satisfactory accuracy.

In addition, the vertical displacements for the plane model for an elliptical load, calculated according to Equation (3.6), are given in Figure 3.4. The considerably smaller values in comparison with those for discoid loading are created by the lower resulting total force and the altered pressure distribution.

3.3.2.2 Analytical Evaluation of the Amount of Deformation for Loading from a High Pressure System

The deformation of the surface of a plane, homogeneous, isotropic, infinitely extended, elastic half-space is calculated for an elliptical load according to Equations (3.6) and (3.7). The horizontal static tilt change under the influence of a high pressure region in comparison to the case of the unloaded or uniformly loaded half-space is calculated according to

$$\Delta N(0, r) = \frac{du\ (0, r)}{dr} \tag{3.8}$$

Since the calculations are based on linear elastic theory, the same amount of tilt with the opposite sign obtain for a low pressure region with the same pressure distribution but opposite sign.

The model chosen for the analysis (see Figure 3.5) is oriented toward the example of the hundred-year low discussed in Section 3.2. The pressure change in the center of the load amounts to 50 mb; because of the rotation symmetry of the problem the pressure distribution is thus completely determined, given the radius of the loaded surface. The elastic properties of the half-space are described by the same parameters as in Section 3.3.2.1.

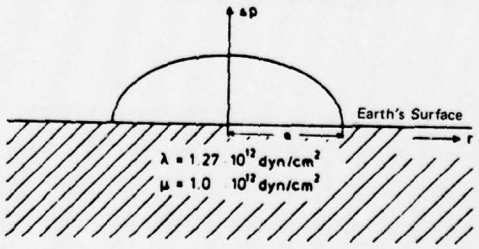


Figure 3.5. Model of the Load Δp with an Elliptical Cross-Section Acting on an Infinitely Extended, Plane, Homogeneous, Isotropic, Elastic Half-Space (λ, μ = Lamé constants; α = radius of the loaded surface)

The results of the calculations are presented in Figure 3.6 in the form of sets of curves $\Delta N = f(r)$ with the radius of the loaded surface as a parameter. The maximum tilts ΔN appear near the edge of the loaded surface and may be given as $\Delta N = 5.8 \cdot 10^{-3}$" irrespective of the radius of the loaded surface. There is one restriction which applies here:

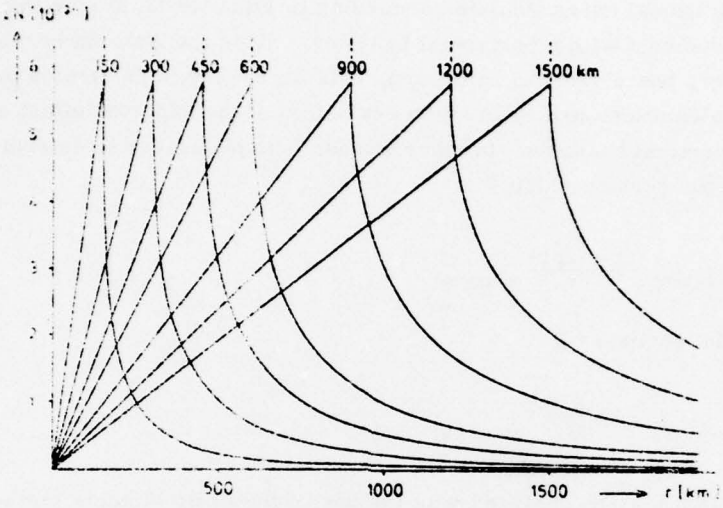


Figure 3.6. The Tilt Change ΔN Resulting from the Deformation Under a Load (see Figure 3.5) as a Function of the Distance r from the Center of the Load, Calculated According to Equation (3.8) (curve parameters: radius α of the load)

The stress distribution for the elliptical load is unspecified at the edge of the loaded surface, that is, for $r = \alpha$. The components of the displacement vector are not defined at this point (see Equations (3.6) and (3.7)). The tilts calculated from them are multi-valued at the point $r = \alpha$. Since the model for the load in this region does not reproduce the actually continuous pressure curve properly, a narrow region (±5 km) around the point $r = \alpha$, in which the instability occurs, is not considered for the analysis of the amount of deformation.

The elastic properties which are used in the calculation are representative of the upper mantle. Since the depth of penetration increases with increasing load radius, with an increasing radius the deformations are determined by the elastic constants of the deeper structures. Thus the maximum tilts for a penetration depth of about 2000 km are reduced to approximately 50 percent of the maximum effect, or $2.9 \cdot 10^{-3}$". In spite of the simple model, therefore, these calculations provide a meaningful evaluation of the maximum observed effects to be expected.

3.3.2.3 Comparison of Horizontal and Vertical Tilts with the Use of the Finite Element Method

From the relationships given in Section 3.3.1.1 it follows that in the case of an analytical solution the transition from the point load to the discoid or elliptical loads is possible only for points calculated on the earth's surface, that is for $z = 0$. The horizontal tilts calculated according to Equation (3.8) give the estimated effect for instruments with a horizontal baseline. Since the Askania borehole tiltmeter, however, has a vertical reference, it is necessary to determine to what extent these calculations are valid as an evaluation of the expected effect on instruments with a vertical baseline. In other words, it is necessary to determine if and how much the horizontal tilt

$$\Delta N(z, r)_{z=\text{const}} = \frac{du\,(z, r)}{dr}_{z=\text{const}} \tag{3.9}$$

differs from the vertical tilt

$$\Delta N(z, r)_{r=\text{const}} = \frac{dv\,(z, r)}{dz}_{r=\text{const}} \tag{3.10}$$

This problem may be analyzed with the use of the finite element method (see Section 3.3.1.2). Because of the finite length of the elements, the differentials in Equations (3.9) and (3.10) are to be replaced by difference quotients for the calculation of the tilts from the nodal point displacements. The simulation of the Boussinesq problem with a three-dimensional finite element model provides, in addition to the vertical tilts, information about how well the numerical solution agrees with the analytical solution for the horizontal tilts. The essential problem here is to simulate the infinitely extended half-space. These relationships are reproduced correctly when the extent of the model is about 50 times the radius of the loaded surface. As the pressure distribution of a discoid load may be given exactly for the analytical and numerical solution (approximation errors arise in the case of the numerical solution for the elliptical load), the model of the discoid load is chosen for this comparison.

The results are presented in Figure 3.6. The horizontal tilts calculated according to the Boussinesq method and with the SAP IV finite element program show that the analytical and numerical techniques yield almost identical results. The vertical tilt changes (the tilts are given at a depth of 25 m) are everywhere smaller than, or equal to, the horizontal tilt changes. Near the edge of the loaded surface ($\alpha = 150$ m) the vertical tilts are smaller than the horizontal ones by a factor of 2.

At greater distances from the center of the load the two curves approach each other; from about 3α, horizontal and vertical tilts can be considered identical. These results are valid for any α. The calculations show that the maximum values for the amount of deformation calculated in Section 3.3.2.2 actually are to be viewed as the upper limit. The vertical tilt changes may be up to 50 percent smaller than the horizontal ones; the exact ratio of the two effects is determined by Poisson's ratio.

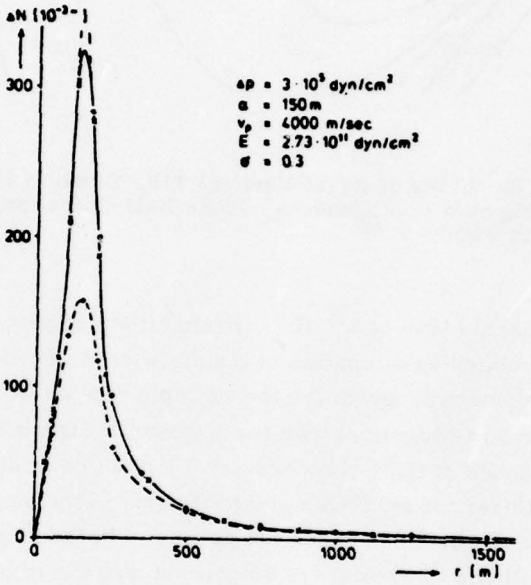


Figure 3.7. Comparison of the Horizontal Tilts Calculated According to the Boussinesq Method (-o-o-) and the Finite Element Method (-x-x-) with the Vertical Tilt Changes Calculated by Means of the FEM for a Discoid Load

3.3.2.4 Depth Dependence of Tilt for Surface Loads

The problem of depth dependence of tilt plays an important role in the interpretation of the data since this gives an effective criterion for the selection of models which are compatible with the measurements. Since this problem appears several times in the course of the study, the relationship will be discussed briefly here.

Figure 3.8 shows the decrease in vertical tilt with depth.

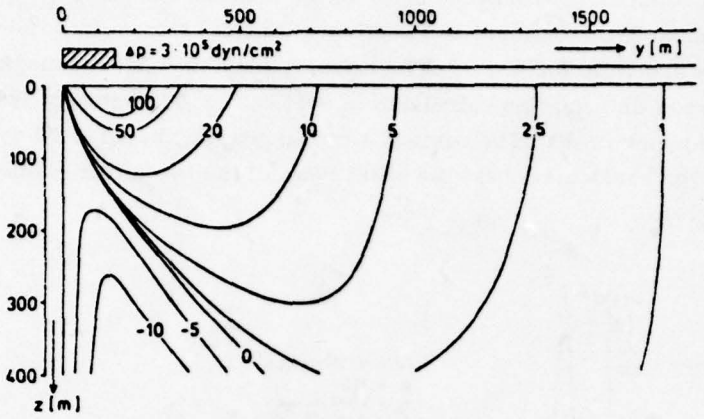


Figure 3.8. Lines of Equal Vertical Tilt, Given in 10^{-3}", for Loading on a Homogeneous, Plane Half-Space (parameters as in Figure 3.6)

The effect of a discoid load of $3 \cdot 10^5$ dyn/cm^2 (the radius of the loaded surface is 150 m) is calculated as a function of the distance r and the depth z by means of the SAP IV finite element program for the example treated in Section 3.3.2.3. The elastic parameters are identical with those given in Figure 3.7.

The depth dependence of tilt is, accordingly, a function of distance from the center of the load. Under the load even small changes in the observation depth may lead to tilt changes which can reach 100 percent. In the region outside of the load, changes in amplitude of about 20 to 30 percent are possible for a variation of 15 m in the measurement depth. At a distance of about 5α the depth dependence of the effect becomes negligibly small; the lines of equal tilt here run approximately vertically near the ground surface.

This example is directly applicable for the evaluation of the tilt effect and its depth dependence, as, for example, that may appear in the case of load changes from water level fluctuations in lakes and ponds in the area of the Zellerfeld-Mühlenhöhe Station (see Section 5.2). To convert the results to the effect of extensive atmospheric pressure fluctuations, it is only necessary to replace the unit meters in Figure 3.8 by kilometers. For the calculation of tilts it was necessary to use an elastic model appropriate to this spatial dimension; the lines of equal tilt are not, however, influenced by this.

The depth dependence of tilt variations which appear as the result of barometric loading changes over regions several km in diameter, therefore, may be ignored. Insofar as the tilt effects are at all measurable, they are recorded with equal amplitude at depths of 15 m and 30 m.

3.3.3 EVALUATION OF THE ATTRACTION EFFECT

Air pressure depends upon the vertical variation of density, and this in turn depends on the vertical variation of temperature. Air pressure fluctuations, therefore, are caused by the variation in the vertical density pattern over time, so that no unambiguous conclusions about the variation of density with altitude with respect to time may be drawn from the pressure variation on the ground.

However, an understanding of this complicated behavior, which changes according to the prevailing weather conditions, is not necessary for an analysis of the attraction effect which appears as a result of the changed density variation with altitude. The simplifying assumption that the air pressure variation results from a pressure variation constant over the entire altitude range is sufficient. The limit of the density change over the center of the load is assumed to be at an altitude of 5 km; thus, it approaches the pressure distribution on the earth's surface (see Figure 3.5). This distribution results from the fact that the air pressure variations take place in the lower region of the troposphere, the weather-producing layer of the atmosphere (Fortak[33]). Further, it ensures that, especially at the edge of the loaded surface, the maximum attraction effects are calculated.

The changed density distribution over the loaded surface creates a change in the acceleration due to gravity on the earth's surface, the horizontal component of which creates a tilt change in the vertical pendulum. The evaluation of the maximum tilt effect is carried out for the extreme case of the so-called hundred-year low presented in Figure 3.5. One-half of the ellipsoid of rotation in which the density variation takes place is approximated by a polyhedron with eighty-five surfaces. The horizontal component of gravitational effect is calculated according to Götze's[34] method, and the result is presented in Figure 3.9 as a function of the distance from the center of the load with the radius of the loaded surface as a parameter. The maximum tilt effects resulting from attraction appear at the edge of the loaded surface and may be given as $3.6 \cdot 10^{-3}$", essentially independent of of the radius; the small fluctuations of the maximum tilts are to be attributed to the increasing errors with increasing radius for the approximation of the ellipsoid of rotation. Outside of the loaded surface the tilt changes due to attraction decrease approximately proportional to $1/r^2$ ab.

---

33. Fortak, H. (1971) Meteorology, Carl Habel Publishers, Berlin and Darmstadt.
34. Götze, H.-J. (1976) A Numerical Procedure for Calculating the Gravimentric and Magnetic Field Values for Three-dimensional Models, Diss. TU Clausthal.

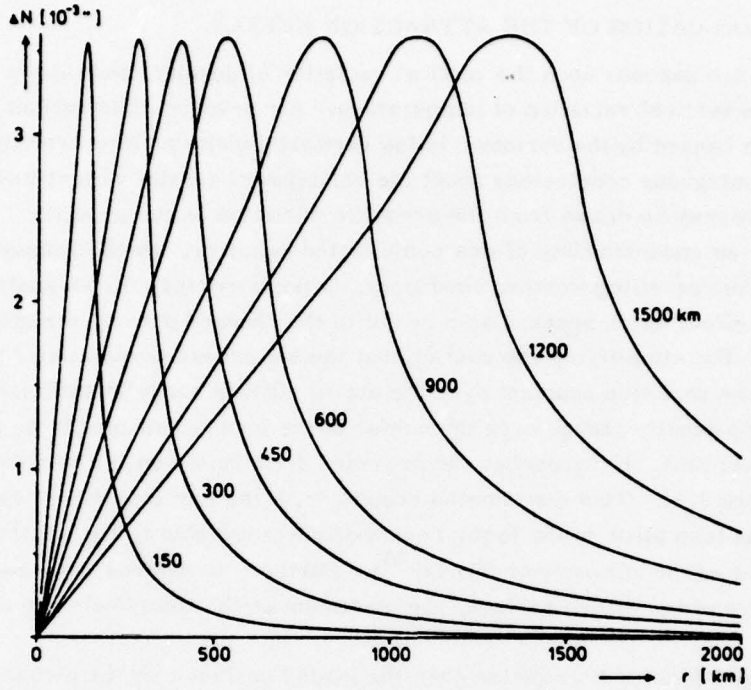


Figure 3.9. Attraction-Caused Tilts ΔN Due to a Changed Density Distribution in the Atmosphere as a Function of the Distance r from the Center of the Load with the Radius α of the Loaded Surface as a Parameter

3.3.4 SUMMARY OF RESULTS

The analysis of the amount of deformation carried out for the horizontal tilt changes indicates a maximum tilt change of about $5.8 \cdot 10^{-3}$", while that of the attraction portion is about $3.6 \cdot 10^{-3}$" near the edge of the loaded surface. The two amounts are added together, so that a total effect of $9.4 \cdot 10^{-3}$" can appear for an air pressure change of 50 mb. In view of the fact that the vertical tilts may be up to 50 percent smaller than the horizontal tilts which are used for this analysis, it is certain that an upper limit for the possible tilt effects is actually given here.

The findings which result from the qualitative investigation of the tilt behavior during the hundred-year low are confirmed by the results of the model calculations. Both with respect to the tilt amplitude and to the depth dependence of the tilts, the model calculations show that air pressure influences are to be excluded as the cause of the disturbance in the tilt recordings on 9-10 February 1974. The tilt

signal to be expected according to the calculations during the air pressure drop cannot be identified in the recording (Figure 3.2) which indicates that the measured effects are still clearly smaller than the calculated ones. The signal-to-noise ratio for tilts caused by air pressure (it is about 1:20 or 1:10 according to the depth of measurement) is so unfavorable that further investigation of these signals appears to be of little promise. Also, as the discussion in Section 4.4 shows, this ratio probably cannot be significantly improved.

Thus, for example, the possibility of using tilts resulting from air pressure for solving geodynamic problems such as the structure of the crust and of the upper mantle is excluded. In addition to the unfavorable signal-to-noise ratio, the uncertainty in the vertical pressure variation is decisive here. Although this information can be found precisely from meteorological weather maps, it must be clarified by model calculations.

4. THE INFLUENCE OF LOCAL PRECIPITATION ON TILT MEASUREMENTS

4.1 Empirical Correlation between the Amount of Precipitation and Tilt

The discussion of the tilt characteristics during the so-called hundred-year low (see Section 3.2) makes it clear that the tilts occurring during this period (see Figure 3.2) are not causally connected with air pressure variations. Two further meteorological influences, namely the amount of precipitation per unit time and the air pressure for the same time period as in Figure 3.2, are presented in Figure 4.1 for a further investigation of the tilt changes. The tilt variation from 5 February to 8 February 1974 shows that precipitation in the form of snow does not measurably influence the tilt measurements, especially not if the air temperature is about $0^{\circ}C$. Load effects from the snow cover, therefore, are of a negligible magnitude (see Section 4.3). By the beginning of 9 February the snow turned to rain, the air temperature rose above $0^{\circ}C$, and a snow cover several centimeters deep began to melt. A short time later a rapid drift in the two tiltmeters began, continuing almost to the end of the precipitation signal; finally, both components of the tiltmeters moved toward their original position. The penetration of water into the ground as a consequence of rain or as the result of thawing periods, therefore, led to characteristic tilt signals.

In order to check this result, the amount of precipitation per day (climatic data from the Clausthal-Zellerfeld Weather Station) and the tilts are presented in Figure 4.2 for a period of eight months. Greater amounts of precipitation in the form of rain thus are correlated with larger tilts. The tilts clearly decrease with the depth. By measuring the maximum deviations the amplitude ratio between the tilt changes measured at depths of 15 and 30 m are found to be approximately 2:1,

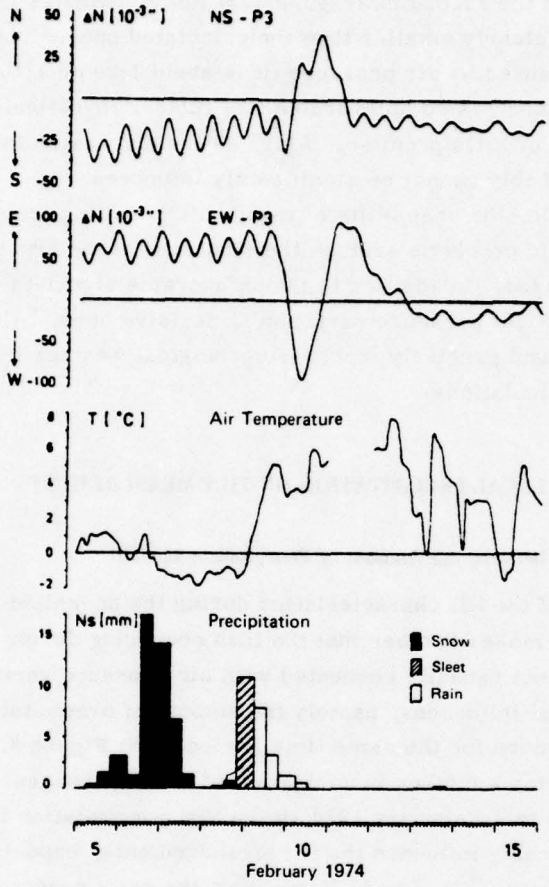


Figure 4.1. Connection Between the Tilt Change Due to Air Temperature T and Precipitation Ns (given with respect to the time interval between the meteorological recording times 0700, 1400, 2100; precipitation and temperature data: Clausthal-Zellerfeld Weather Station)

fluctuating between 1.5:1 and 2.5:1. Representative values for the amplitudes are $100 \cdot 10^{-3}$" at a depth of 15 m and $50 \cdot 10^{-3}$" at a depth of 30 m.

The time history of the signals is very similar with the appearance of rainfall, the depth indeed determining the amplitude, but having hardly any influence on the tilt rate with respect to time. Figure 4.3 illustrates the details. A short time after the onset of the rain the component of the tiltmeter shown began to drift rapidly; this process continued for several hours past the end of the rain signal. Finally, when no new precipitation occurred the tilt signal faded away with a

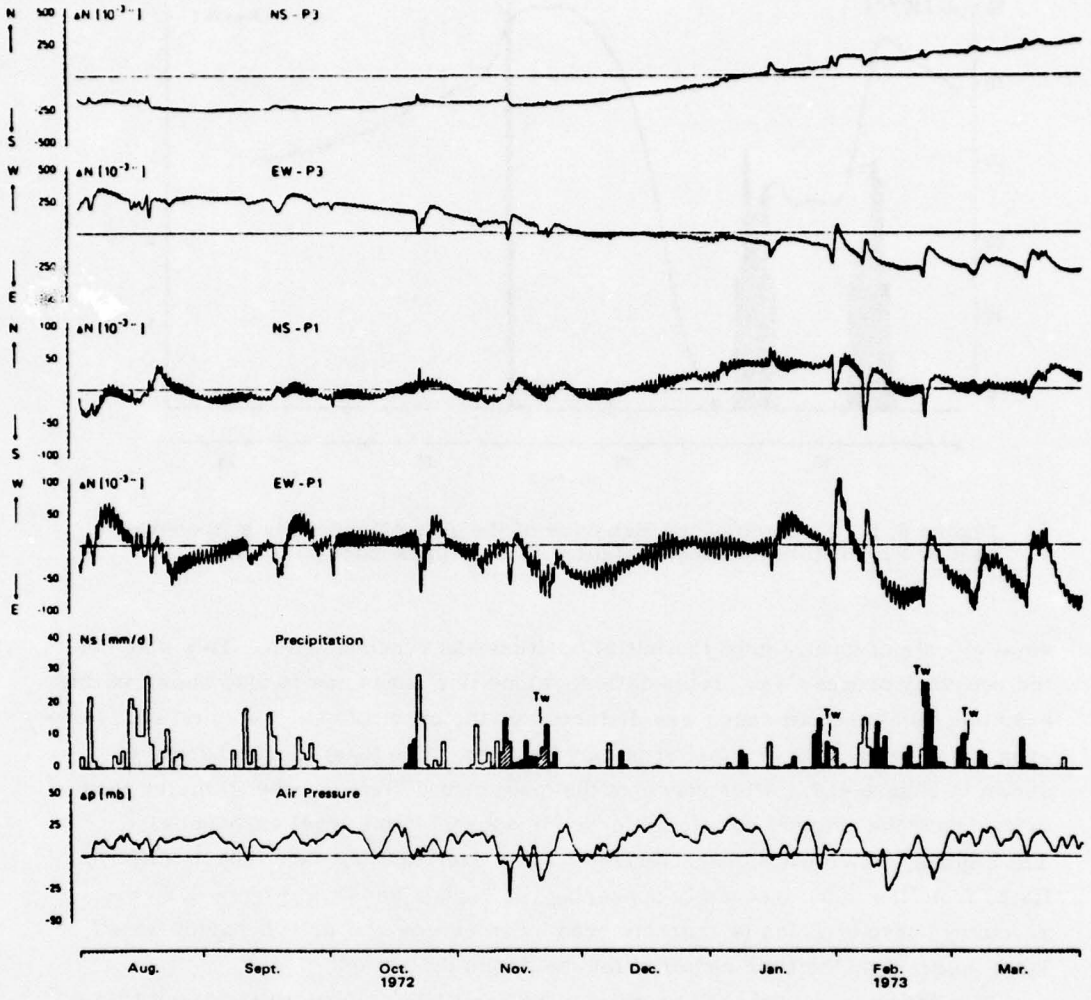


Figure 4.2. Influence of Precipitation (symbols as in Figure 4.1) and Melting Phase (Tw) on Tilt; Comparison of the Local Air Pressure Variation with the Amount of Precipitation per Day (installation depth: P1 = 30 m; P3 = 15 m)

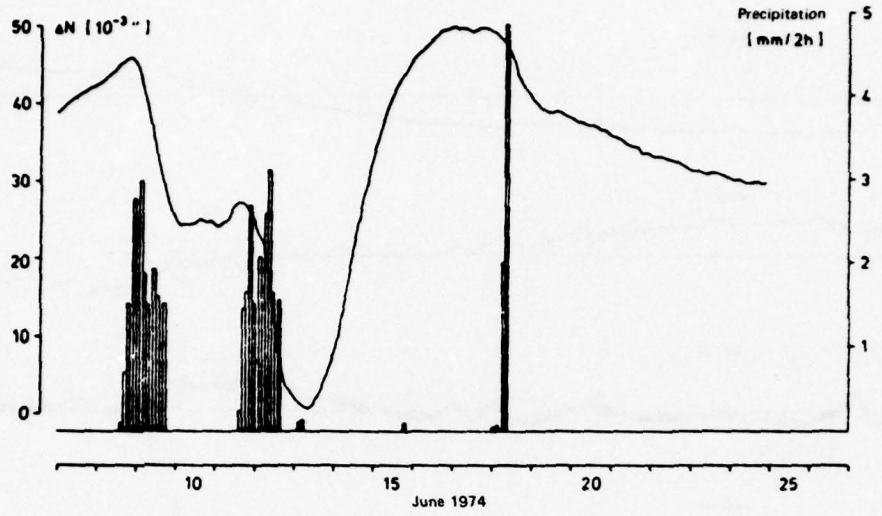


Figure 4.3. Example of the Behavior of the Tilt ΔN over Time (x component of P1, installation depth 30 m) with the Appearance of Rainfall

smaller rate of change until the initial position was reached again. This stage of the recovery process was problematical, since this phase, as is also shown in this example, in almost all cases was disturbed by the onset of new precipitation. However, two typical recovery patterns may be cited. The least frequent form is shown in Figure 4.3. After reaching the maximum deflection, the tiltmeter then drifted past the original position in order to approach this level exponentially. The signals, which were characterized by this overshooting, are clearly differentiated from the more frequently appearing tilt signals shown in Figure 4.5, the recovery phase of which is characterized by an exponential drift behavior which lasts longer than the time required for maximum deflection.

The description of the tilt signals in the period from January to March 1973 is considerably complicated by the complex interaction of the meteorological parameters, and therefore these signals will be discussed only briefly here. In Figure 4.1 it has already been shown that precipitation in the form of snow creates no measurable tilt. This fact is also demonstrated in Figure 4.2 with several examples. Tilt effects appear only when the snow cover thaws; this phase is characterized by an increase in the air and ground temperature to over $0^{\circ}C$. The transition from snow to sleet to pure rain is a frequently occurring phenomenon. From time to time the thawing period, which first produces a tilt change, is interrupted by a freezing period, for example, as is shown in Figure 4.2 on 31 January 1973

and on 22 February 1973. This effect creates very large tilts, in the EW component of P3 up to $300 \cdot 10^{-3}$", which clearly differ from the tilt signals otherwise appearing in connection with precipitation.

In addition, the air pressure variation is shown in the lower part of Figure 4.2 for illustrating the results of previous studies (Herbst[17]). A comparison with the precipitation makes it clear how a significant correlation between air pressure and tilt may appear indirectly; since precipitation frequently is the result of low pressure influences, and, therefore, as there is a significant correlation between air pressure and precipitation, the correlation between air pressure and tilt also is frequently significant for short periods of time. Only the greatly fluctuating phase data indicate the apparent correlation is not worth interpreting.

4.2 Quantitative Investigations

The results of the qualitative evaluation of the data in Section 4.1 make a more detailed investigation appear promising. The characteristic form of the tilt signals caused by rainfall indicates that these signals possibly are predictable by means of the measured variable amount of precipitation per unit time. Next it is assumed that the tilt-precipitation system can be completely described by a linear transfer function. Therefore, except for the assumption of a linear system, no assumptions are made about the physical model. A knowledge of the transfer function would make a filtering of the measurements for precipitation effects possible. This would make possible investigations of tilt-inducing effects which are an order of magnitude smaller, such as, for example, long-period tides and air pressure effects.

4.2.1 EXPERIMENTAL PREREQUISITES

The most exact measurement of the precipitation possible with a precise time resolution is a prerequisite for the numerical investigation of the precipitation-tilt system. The previously used data of the Clausthal Weather Station do not satisfy this requirement. Therefore, a rain gauge (Thies Co., Göttingen, type 4031.10) which operates according to the drop counter principle was installed at the Zellerfeld-Mühlenhöhe Station. A nozzle from which drops of a specific volume separate is located at the lowest point of a downward tapering standardized collecting cone. A drop corresponds to 0.005 mm of precipitation. The separating drops interrupt a light beam, each drop triggering a pulse. The number of the pulses is counted and recorded, and it can be retrieved at any time. Thermostatically controlled heating of the collecting cone also ensures that the precipitation gauge is capable of operating at temperatures below 0°C. Precipitation falling as snow thaws immediately and the equivalent amount of precipitation can be measured.

Measurements of the amount of precipitation at 12-minute intervals are available for the period from May 1974 to July 1975.

4.2.2 PREDICTION OF THE TILT SIGNAL BY THE AMOUNT OF PRECIPITATION PER UNIT TIME

First of all, of the many possible model representations (see Section 4.3) a linear transformation system w(t) between the input variable x(t) (amount of precipitation per unit time) and the output variable y(t) is postulated as in Figure 4.4, that is, no information about the actual effective mechanisms is assumed. Since first of all we are concerned with a filtering of the tilt recordings in order to separate out signals resulting from precipitation, this procedure appears to lead to the goal the fastest.

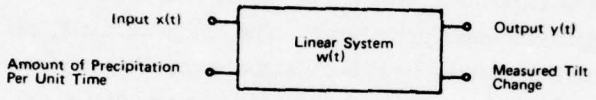


Figure 4.4. Description of the Connection Between Amount of Precipitation and Tilt Change by Means of a Linear System

For the linear system of Figure 4.4 we have (Kanasewich[35])

$$y(t) = \int_0^\infty w(\tau) \cdot x(t - \tau)\, d\tau \qquad (4.1)$$

where w(t) is the impulse response of the system, and τ is the time shift. The output signal y(t), therefore, is predictable by the convolution of x(t) and w(t) in the time domain assuming knowledge of the impulse response w(t) and the input signal x(t). If x(t) and y(t) are Fourier-transformable, then the impulse response w(t) can be calculated. From the complex spectra of the input and output functions $X(\omega)$ and $Y(\omega)$ we have the transfer function $W(\omega)$ in the frequency domain

$$W(\omega) = \frac{Y(\omega)}{X(\omega)} \qquad (4.2)$$

---

35. Kanasewich, E. R. (1973) Time Sequence Analysis in Geophysics, The University of Alberta Press.

from which w(t) is obtained by inverse transformation into the time domain. The filtering is performed in such a way that the output signal y(t) is predicted according to Equation (4.1) and then is subtracted from the measured tilt signal.

This method is used successfully by Tanaka[16] for predicting the tilt signals caused by precipitation. On the other hand, applying it to the precipitation and tilt data measured at the Zellerfeld-Mühlenhöhe Station provides no usable results. The reasons for this are, in particular, that a fundamental prerequisite for the use of the process is not present. Namely, there is not a sufficient number of undistorted tilt signals present, undistorted being used here in the sense that, outside of the one signal caused by precipitation to be analyzed, no further distorations are present. This also means that no additional precipitation signals should appear before the tilt signal to be analyzed has completely faded away. The complex spectra of the transfer function $W(\omega)$ from different time intervals, calculated with the available data, display great deviations from one another in such a way that the averaging and smoothing of the spectra necessary for an unambiguous determination of w(t) is not possible. The large deviations of the calculated spectra from one another may be seen as an indication that the functional connection, as it is described by Equation (4.1), may not always be valid.

A deterministic procedure for determining the impulse response in the time domain is used below in order to check to what extent the method of determining the impulse response and the nonoptimal prerequisites with respect to undistorted data are responsible for the result, the investigation being limited to tilt signals which display no overshoot (see Section 4.1). We proceed under the assumption that the impulse response is unknown as to type and may be represented by a function of the following form:

$$w(t) = \alpha \cdot t^{\beta} \cdot \exp(-\gamma \cdot t^{\delta}) \tag{4.3}$$

where α, β, γ, and δ are parameters which are adjusted to obtain an optimal fit of the predicted tilts with the measured tilts. The sum of the standard deviations is used as a measure of the agreement. The calculations are again carried out for individual signals caused by precipitation. Representative average values are to be determined by a subsequent averaging of the values of α, β, γ, and δ from many random samples. Filtering of the measured tilts precedes these calculations in order to eliminate the tides and long-period drift.

The result is presented in Figure 4.5. It shows that the problems are similar to those encountered in the previously described attempt to determine the actual relationships with the procedure for a linear system which results from the calculation of the impulse response according to Equation (4.2). Comparison of the predicted and measured tilts for the period from 1 October to 19 October 1974

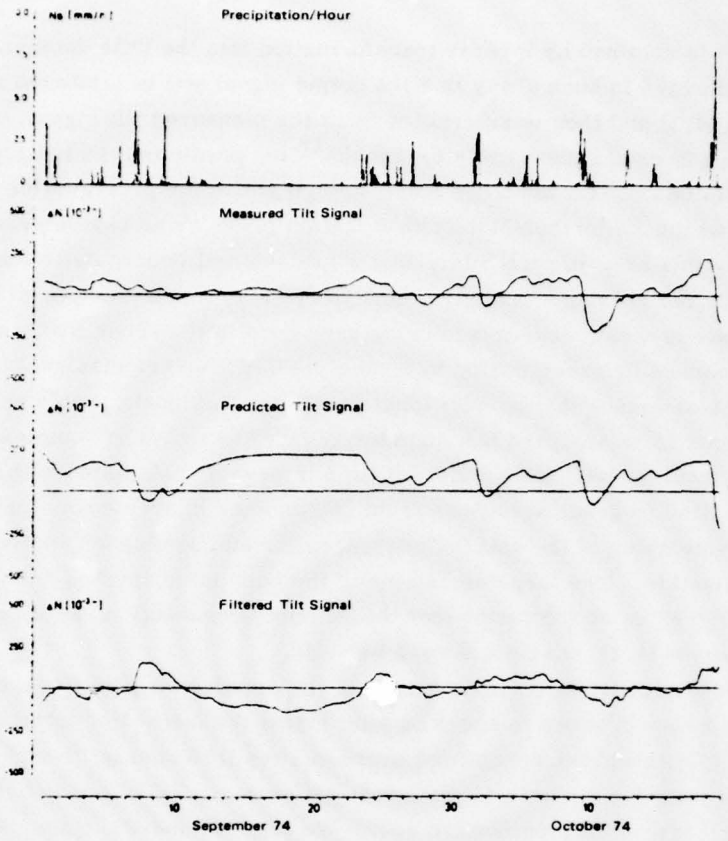


Figure 4.5. Result of the Prediction of the Tilt Signal ΔN with the Use of the Parameter: Amount of Precipitation per Hour Ns (mm/h)

shows that it is basically feasible to obtain the impulse response w(t) of the system in the form of Equation (4.3) for individual cases. The use of this impulse response with the same parameters for the precipitation signal of the month of September, on the other hand, produces not even a close approximation of the measured tilts. It is especially striking here that the tilt signals which appear at the end of September after a long dry period are significantly smaller than should be expected according to the measured amount of precipitation. This indicates that the prehistory of the event must also be considered.

The use of the two methods shows that there is no impulse response representative of all precipitation events; that is, the simple functional relation between the amount of rain and the tilt change according to the form given in Equation (4.1) does not reproduce the physical processes. The relationships are apparently

considerably more complicated, so that the goal of optimally filtering the measured tilts for rain effects cannot be achieved with the use of the procedures discussed. The following factors come into consideration as possible causes:

- The mechanism is that of a linear system; however, a description of the process using the amount of rain per unit time is not sufficient. Further parameters, which in general are not amenable to measurement, play a role; these include, for example, the ground moisture or degree of saturation of the ground and the rain temperature.
- Nonlinearities appear in the precipitation-tilt system, for example, nonlinearities resulting from ground saturation effects.
- The amount of rain per unit time is correlated with the actual causal factors such as, for example, water level fluctuations in the subsoil; the connection between the two is nonlinear, for example, because of partial surface runoff (see Section 4.3.4.3).

No further statistical analysis would appear to be promising, since the multiplicity of possibilities and the complexity of the effective mechanisms are too great.

4.2.3 INFLUENCE OF THE PRECIPITATION SIGNAL ON THE ANALYSIS OF THE TIDES

Finally, we will deal briefly with the influence of the tilt signals created by precipitation on the results of an analysis of the tidal tilts. Fourier analysis of the tilt signal predicted by means of Equation (3.3) shows that for the 12- and 24-hour tide wave groups in each case we have to reckon with a distortion of the tidal amplitudes of the order of magnitude of up to $1 \cdot 10^{-3}$". This statement is based on the fact that a single tilt signal due to precipitation appears in the data interval analyzed. This tilt effect, therefore, leads to a non-negligible distortion of the diminishing factor and the phase which is determined essentially by the timing of the precipitation signals. More exact specifications cannot be made because of the inadequate approximation of the precipitation signals.

4.3 Discussion of Different Model Concepts

A formal description of the connection between precipitation and tilt with deterministic and statistical means is not possible according to Section 4.2.2. A classification of the precipitation events according to the other climatological factors such as air temperature, ground temperature, ground moisture, and so forth, possibly could produce progress here. However, such a classification fails because of insufficient information about the behavior of these factors since, for example, the ground conditions are only roughly classified in the weather data. Another complication is the fact that the number of precipitation signals appearing

under identical conditions is so small, because of the seasonal weather changes, that it is not sufficient for a statistical analysis.

From the multiplicity of possible reasons for the failure of the attempts indicated in Section 4.2.2, it must be concluded that the only remaining possibility for obtaining a description of the connection between precipitation and tilt comes from the development of appropriate model representations of the effective mechanisms. The following information taken from the observed data is used as criteria for the selection of an appropriate model:

- the ratio between the tilt changes measured at 15 m and 30 m deep amounts to around 2:1 at the time of maximum tilt change;
- representative values for the amplitudes are $100 \cdot 10^{-3}$" and $50 \cdot 10^{-3}$";
- the time history of the tilt signal explained in greater detail in Section 4.1;
- the preferential direction of the resulting tilt signal, which lies at about $80^{\circ}N \pm 10^{\circ}$ (Flach et al[19]).

Finally, different possible causal factors should be considered. Appropriate models for these should be developed and, as far as possible, checked numerically.

4.3.1 HEAT TRANSFER THROUGH PRECIPITATION

Energy transfer from the atmosphere to the earth, in particular the transfer of heat energy, is connected with the occurrence of precipitation. The temperature of the precipitation, which generally deviates from the existing ground temperature, leads to temperature fluctuations in the surficial ground layers down to depths of several decimeters. However, according to results in Section 5.1.5.2, these are incapable of creating thermoelastic disturbances of the order of magnitude of the measured tilts. The small depth of penetration of these temperature changes is confirmed by the results of the temperature measurements at depths of 4.5 and 7 m. The measurements are made with platinum wire probes and provide a resolution of about $0.01^{\circ}C$. They show that no measurable temperature changes appear at these depths during rainfall.

Because of the fact that the graywacke in which the boreholes are located is highly subject to fracturing, there is, however, the possibility that the water penetrates to greater depths very rapidly through the cracks, the widths of which are in the cm to dm range near the surface, since the cracks offer a very low resistance to the water flow. The thin layers of graywacke shale and clay shale embedded in the Culm graywacke act in part as damming layers; that is, they hinder a penetration of the water to greater depths. The permeability across the impermeable layers is smaller in comparison to that of the cracks by several orders of magnitude, so that the maximum temperature equilibration between the water and surrounding rock takes place in the region of these damming layers. The resulting temperature fluctuations in connection with the topography (see Section 5.1.5) lead

to thermoelastic distortions in the rock, which again create tilts. This greatly simplified presentation is modelled with a finite element model only slightly different from that described in Section 5.1.5.1, using a closer nodal point spacing in the vicinity of the damming level for a more meaningful temperature approximation. The water conducting layer lies at a depth of 19 m; a temperature difference of 0.1°C, which diminishes to zero at 18 or 20 m, is assumed at this depth according to the left hand part of Figure 4.6. The variation of tilt with depth in the region of the borehole, presented in the right hand part of Figure 4.6, shows that the tilt variations, like their cause, are limited to a very narrow depth range. The tilt effect practically disappears at a distance of 2 m above or below the damming layer. Consequently, this model is not suited to explaining the measured tilt effects in connection with rainfall.

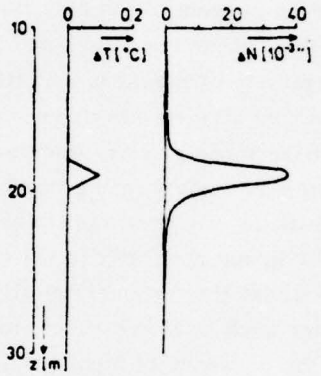


Figure 4.6. Thermoelastically Caused Tilt Changes ΔN for Temperature Changes ΔT in the Region of the Damming Layer

The fact that the rain temperature can be lower or higher than the ground temperature also argues against these thermoelastically caused precipitation effects. Tilt signals of different signs should occur, irrespective of the above-mentioned model, which, however, is not the case with pure rain signals according to Figure 4.2. The internal weakness of this model is also apparent from the following qualitative consideration: namely, it requires that no water stand in the cracks from the ground surface to the impermeable layer, since only in this way could the rain water rapidly reach the region of the damming layer. This assumption does not appear to be realistic (see Section 4.3.4).

4.3.2 EXPANSION EFFECTS FROM CLAY MINERALS

A further model concept is connected with expansion processes. These may take place in the area of the surficial layer or in the filling of cracks or gangue intrusions. Clay materials, which increase their volume when they absorb water, are involved in these swelling effects. These result in disturbances in the vicinity of the earth's surface which may possibly operate to the depths at which the tiltmeters are installed.

Next it is possible to show with the finite element model for the Zellerfeld-Mühlenhöhe Station described in Section 5.1.5.1 that the volume changes in the regolith and in the weathered graywacke may lead to tilt changes of the order of magnitude observed. If we assume a water-absorbing clay mineral proportion of about 1 percent in the weathered layer, which decreases linearly downward to 0 percent at the solid graywacke, and we assume that the swelling processes create a volume increase of about 50 percent of the clay fraction, we obtain tilt effects of about $100 \cdot 10^{-3}$" at a depth of about 15 meters and $70 \cdot 10^{-3}$" at a depth of about 30 meters. Thus, the magnitude of the measured tilt effects is well approximated.

The clay materials may be divided into three large groups: montmorillonite, illite, and kaolinite. Of these three groups, montmorillonite possesses the property of increasing its volume by incorporating water molecules into the crystal lattice and adsorbing interstitial water by multiples of its volume in the dry state. On the other hand, the illite group generally is not capable of swelling, and the kaolinite group does not possess this property at all (Villwock,[36] Philipsborn[37]).

The question of whether such swelling effects may or may not appear, therefore, reduces to whether the presence of montmorillonite is probable in the region of the Zellerfeld-Mühlenhöhe Station. According to Betechtin[38] montmorillonite appears as a product of weathering of basic volcanic rocks. This prerequisite is not met in the region of the Clausthal Culm fault zone. This opinion is also confirmed by geological studies (Mohr, 1976, personal communication), which give no indication of the existence of montmorillonites.

From the time history of the tilt signal caused by precipitation it must further be concluded that we are dealing with a completely reversible process. The volume increase created by the incorporation of water molecules, therefore, insofar as further water flow is concerned, must reverse slowly because of drying until the initial volume is again reached in about 20 days. In this case the variable portion

---

36. Villwock, R. (1966) Industrial Geology, Stein Press, Offenbach/Main.

37. Philipsborn, H. von (1967) Tables for Identifying Minerals According to External Geological Features, E. Schweizerbart's Publishing Company, Stuttgart.

38. Betechtin, A. G. (1968) Lehrbuch der speziellen Mineralogie, VEB Deutscher Verlag für Grundstoffindustrie, Leipzig.

of the incorporated water is determined by the interstitial water, which can be removed by air drying; on the other hand, the water of crystalization may be removed only by temperatures of several hundred degrees centigrade (Grim[39]).

The concept that the variable portion of the interstitial water determines the volume changes of the clay fraction and thus also the tilts is, however, not consistent with two observations. In the first place, in months with heavy precipitation and low rates of evaporation, we have to deal with a very high ground moisture content, which, apart from the immediate ground surface, is relatively constant. Drying out and, therefore, a reduction of the interstitial water cannot be assumed; the process is not reversible. On the other hand, saturation effects must appear in the case of high amounts of precipitation or closely following occurrences of precipitation which result in the fact that the swelling, and thus the volume change, reaches its maximum. Further precipitation, therefore, should not create any tilt changes. Such saturation effects, however, have not been recorded up to the present time.

These considerations, together with the small probability of the existence of clay minerals capable of swelling at all, show that an interpretation of the tilt signals by these expansion mechanisms is not possible.

4.3.3 LOAD EFFECTS FROM PRECIPITATION

The question of whether the tilts measured in connection with precipitation may be interpreted by loading effects may be answered by special calculations with the use of currently available data.

Figure 4.1 clearly indicates that precipitation in the form of snow creates no measurable change in tilt. The effective load in this case may be specified directly: the snowfall from 5 February to 7 February 1974 is equivalent to 56 mm of rain. If this amount of precipitation had fallen in the form of rain, according to experience there would appear a tilt signal with an amplitude of over $100 \cdot 10^{-3}$" (see Figure 4.2). In the case of the same amount of precipitation and a correspondingly equal load the tiltmeters behave completely differently. Thus, the load effect cannot be responsible for the measured tilt.

This result is confirmed by a numerical evaluation with the use of the finite element model described in Section 5.1.5.1, which considers the topography of the area around the station.

Since the amount of precipitation on the surface covered by the model can be viewed as approximately constant, we can use a constant loading of the surface of the model in our calculations. No tilts appear in the case of flat topography and horizontal geological strata; because of the undulating topography, however,

---

39. Grim, R.E. (1953) Clay Minerology, McGraw-Hill, New York.

strain-induced tilts are created. Therefore, in the case of a load of 10 mm of precipitation and a maximum topographic slope of 10 percent, the calculations give tilt changes on the order of $0.01 \cdot 10^{-3}$" at a depth of 15 m, a value which can not be resolved by the Askania borehole tiltmeter and its recording system.

Unequal loading of the earth's surface could be produced by the accumulation of precipitation in low-lying areas as, for example, in the vicinity of Stadtweger Pond (see Figure 2.1). However, this also cannot be considered a cause, since, as Figure 5.9 shows, completely unrealistic assumptions would have to be made about the loads in this case. These would have to be of the order of $3 \cdot 10^5$ dyn/cm^2, which corresponds to a pressure exerted by 3 m of water. In addition, this concept is not compatible with the depth dependence of the tilt effects discussed in Section 3.3.2.4.

4.3.4 LATERAL FLUCTUATIONS OF THE FRACTURE WATER LEVEL

4.3.4.1 Geological Description of the Fracture System

Flach et al[19] established a preferential direction for the tilt in a narrow angular range around the EW direction in the period range of about 1 to 20 days. Apparently it is connected with the geological structures of the Clausthal Culm fault zone, which are characterized according to Hinze[23] and Mohr[22] briefly as follows: one of the dominant elements is the fracturing which very frequently follows a direction between 100° and 150°. The fractures dip from 60° to 80° to the northeast and to the southwest with approximately the same frequency. They are almost always smooth-walled. Near the surface, they serve as preferred joints, at the most 1 to 3 dm apart. Occasionally they are closer, and more rarely they are farther apart. The width of the joints in the rock depends largely on the pressure of the overlying layers. This means that most of the deep rock joints are closed under high pressure, and, therefore, the rock is nearly impermeable to water. Closer to the surface, that is with decreasing pressure of the overlaying layers, the joints are increasingly open. Thus, it is possible to have ground water flow and the formation of a body of fracture water, the surface of which is regulated by the neighboring valleys and springs.

The unconsolidated zone near the surface is divided into two sections: an upper section a few meters thick, in which disintegration by chemical weathering originating from the fractures prevails, and a lower section, in which the joints are open considerably less frequently and to a lesser extent. In general, this lower region extends to a depth of 40 to 60 m.

4.3.4.2 Model of the Fracture System and Results of the Tilt Calculations

The water level of the body of fracture water is subject to variations with time, for example, as a consequence of precipitation. These variations can change

laterally under the proper conditions (see Section 4.3.4.3). The resulting pressure differences in the fracture system may lead to elastic bending of the rock formation. With respect to the tilt measurements, it must be asked whether and under what conditions it is possible for water level changes in the fracture system to be able to create tilts of the order of magnitude measured.

On the basis of information about the basic geological features of the crack system in the region of the measuring station, a model of a beam stressed on one side is used for evaluating the possible tilt effect (see Figure 4.7). The beam (in the following, it is also frequently called a plate, since the dimension in the x-direction does not enter into the calculation) represents the rock between two fracture surfaces. The clamping depth is identical with the lower end of the fractures (40 to 60 m). The plate thickness corresponds to the fracture spacing, which is most frequently 1 to 3 dm. In the case of different water levels in two neighboring fractures, there is a force which is proportional to the effective pressure difference Δp in the equilibrium state and to the height Δz at which the pressure difference acts.

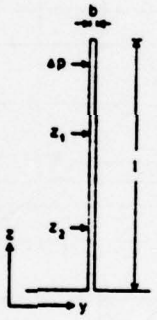


Figure 4.7. Model of a Beam Stressed on One Side

The bending of the beam, the length l of which is assumed to be large compared with the thickness b (dimension in the y-direction), or the resulting tilts, may be calculated analytically (see Macke[40]) according to

$$\Delta N(z) = \tan^{-1} \left\{ - \frac{3\ \Delta p\ \Delta z}{2\ E\ b^3} \left(z \cdot 1 - \frac{z^2}{2} \right) \right\}$$

40. Macke, W. (1967) Particle Mechanics – Systems and Continua, Academic Publishing Company Geest & Portig, Leipzig.

in which E is the modulus of elasticity and z is the distance from the clamping point.

The amplitude ratio of the tilt changes at depths of 15 and 30 m depends only on l since the measurement depths z_1 and z_2 may be expressed by l. If we assume that the forces act near the surface (for example, at a depth of 4 m, that is z_1 = l - 11 and z_2 = l - 26) an effective clamping depth of 35 m is required in order to achieve the measured amplitude ratio of 2:1.

The calculation of the absolute tilt changes is performed for a modulus of elasticity of $1.25 \cdot 10^{11}$ * dyn/cm^2 (see Table 5.4); all other parameters are based on the geological data. Figure 4.8 shows the tilt effect for a depth of 15 m as a function of the thickness b of the rock plates bounded by two fracture surfaces for different effective pressure differences. The group of curves $\Delta N = f(b)_{\Delta p=const}$ shows generally that the solution of the problem is ambiguous; that is, the measured tilts of about $100 \cdot 10^{-3}$" can be realized for different combinations of plate width and pressure difference. For the most probable plate width of 20 to 30 cm,

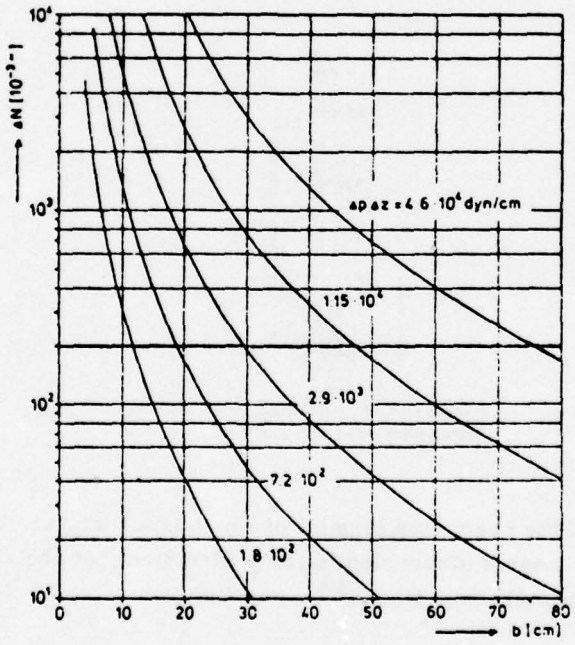


Figure 4.8. Tilt Change ΔN as a Function of the Thickness b of the Rock Plate with Effective Force ($-\Delta p \cdot \Delta z$) as a Parameter (corresponding water level differences: from the bottom 6, 12, 24, 48, 96 mm)

*Erroneously 10^{-3}" in original manuscript.

water level differences of 12 ± 3 mm are required in order to create tilt changes of about $100 \cdot 10^{-3}$" at a depth of 15 m, and $50 \cdot 10^{-3}$" at a depth of 30 m. These water level variations have to appear within a few meters of the earth's surface.

Consequently the calculations show that the tilt effects connected with precipitation can be explained by the mechanism described. Thin rock slabs, with a height of about 40 m and a thickness given by the fracture spacing, bend as a result of forces which appeared in the case of different water level variations in the earth's surface. Since the width of the fractures amounts to several thousanths of a meter, and since the horizontal displacements at the surface are only of the order of magnitude of 10^{-5} m, the precondition of free mobility is fulfilled; limiting aspects are discussed in Section 4.3.4.5.

4.3.4.3 Possible Causes of the Lateral Difference in the Fracture System Water Level

Before the further essential features of the signals (as they are described in Section 4.3) can be discussed, it is necessary to determine how these water level changes come about. Several causes, which are outlined below, are conceivable.

The fractured graywacke is overlain with a weathered layer of uniform thickness. This weathered layer exhibits an inhomogeneity in permeability, as is shown schematically in Figure 4.9. With respect to the behavior of the fracture water level, it must be assumed that it lies at a depth of about 4 m and essentially follows the topography, so that the assumption made in Section 4.3.4.2 about the point of application of the effective forces is upheld.

After the onset of rain, a smaller water level change appears under the region with the lower permeability in (2) as compared with (1) (see Figure 4.9). The timing of the maximum water level difference is determined by the ratio of the permeabilities. Finally, a gradual reduction of the pressure differences takes place as a result of a percolation of the water stored in the less permeable region. This behavior is shown qualitatively in Figure 4.9(a). This concept is based on the fact that the permeability in the horizontal direction in the fractured rock is small as compared with the permeability in the weathered layer, so that the equalization processes are negligible in the horizontal direction.

A part of the precipitation can run off on the surface as a result of a sloping topography (see Figure 4.9(b)). The amount is determined by the absorptive capacity and permeability of the ground, the slope, and the individual features of the landscape (Schneider[41]). Because of the surface runoff, more water can percolate into the ground in the region of higher permeability than in areas with lower permeability. Different water levels in the fractured rock under these two regions result from this. The difference for points (1) and (2) is shown in Figure 4.9(b).

---

41. Schneider, H. (1973) Water Development, Vulcan-Verlag, Essen.

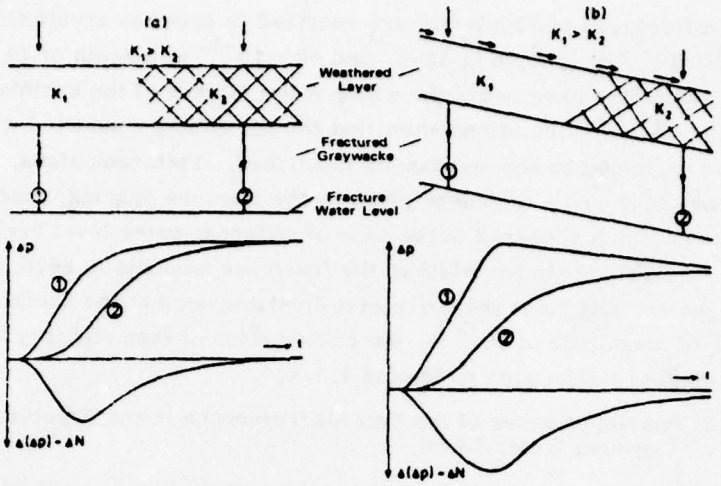


Figure 4.9. Model for the Qualitative Description of the Pressure and, Therefore, Tilt Behavior with Different Permeabilities k_1, k_2 in the Surficial Layer, (a) With a Horizontal Surface, (b) With an Inclined Surface and Surface Runoff ($\Delta(\Delta p)$ = differential pressure between (1) and (2))

The equalization can take place only through layers which are permeable in the horizontal direction; for example, along the clay and graywacke shales. The two portions described reinforce each other, so that the qualitative tilt pattern shown in Figure 4.9(b) results. This concept is particularly suitable for explaining the long decay time of the tilt signal and thus the equalization process in the fractured rock. Of course, it assumes that the tiltmeters must be located upslope from the region with the lower permeability so that a tilt change is always created in the direction of the sloping ground.

The assumption of an inhomogeneity in the permeability does explain the origin of the water level difference in neighboring fractures and its behavior over time. To be sure, such inhomogeneities cannot be excluded; however, they are not geologically certain. Consequently, it appears to be useful to look for more probable model concepts. One approach is to base our considerations on a weathered layer of uniform permeability, the thickness of which increases as it slopes downhill (see Figure 4.10). Two cases are to be differentiated: without surface runoff and with surface runoff (see Figure 4.10). Once the precipitation falling as rain percolates uniformly into the ground no surface runoff occurs. In the region of the greater thickness of the weathered layer ((2)) the water arrives with a delay with respect to (1). This delay depends on the ratio of the thicknesses of (1) and (2). As seen in Figure 4.10(a), this results in a water level difference which

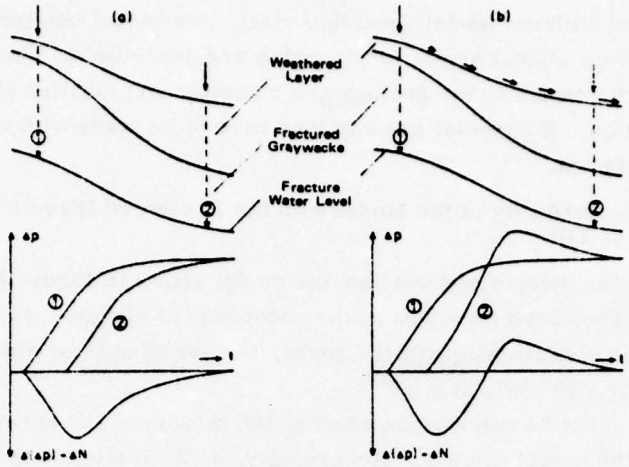


Figure 4.10. Model with Different Thicknesses of the Weathered Layer for a Qualitative Explanation of the Pressure Behavior and the Resulting Tilt Variation, (a) Without Surface Runoff, (b) With Surface Runoff ($\Delta(\Delta p)$ = differential pressure between (1) and (2))

then creates a tilt in the downward direction. Equilibrium conditions are attained when all of the water stored in (2) has reached the fracture water level under the influence of gravity. The disappearance of the tilt signal with time is a function of *the effective* pressure difference between (1) and (2) in each case.

A considerable modification of the tilt signal occurs when, for example, the amount of precipitation per unit time is very high and a portion of the precipitation runs off on the surface. The result of this is that, with a decreasing slope of the land, more and more water can percolate into the ground. To be sure, because of the lesser thickness of the weathered layer in (1) there is at first a pressure rise as compared to (2) (see Figure 4.10(b)); however, this levels out relatively quickly after the precipitation ends. This trend continues with the runoff water which has also penetrated into the ground in the depression, so that now there is a pressure rise in (2) as compared to (1). This pressure difference decreases slowly as a result of the water running off in the direction of the valley or even perpendicular to the fractures, the time required for equalization being determined by the permeability in the horizontal direction. The resulting tilt behavior is characterized by a tilt first in the direction of the topography, and then by a reversal past the original position. In the case of level topography the amount of the overshoot is determined by the water running off the surface and percolating into the ground at lower elevations. The ground then returns to its initial state, as before the onset of the precipitation, comparatively slowly.

As compared with the model described first, this model has the advantage that it explains both typical signal forms which are described in Section 4.1. The assumptions with respect to the geology are plausible and fulfilled at the Zellerfeld-Mühlenhöhe Station. No special assumptions have to be made with respect to the position of the station.

4.3.4.4 Compatibility of the Model with the Preferred Direction of Tilt

It still must be determined whether the model shown in Figure 4.10 is compatible with the preferred direction of the recorded tilt signals. In the plane of the tiltmeters, these produce ellipsoidal figures, the major axes of which have a direction of $80^{\circ}N \pm 10^{\circ}$ (Flach et al[19]).

Further, it must be determined whether the measured tilt agrees with that resulting from the model concept. Accordingly, a tilt in the downward direction must occur with the appearance of the rain and the subsequent change in the fracture water level. In particular this condition is fulfilled for the EW component, in which a tilt in the easterly direction always appears. In this case, the topography determines only that a tilt component must occur in an easterly or westerly direction. Generally, the direction of tilt is controlled by the strike of the fractures, which follows the so-called steep Hercynian direction of about $150^{\circ}N$. The tilts should then appear perpendicular to this direction, that is at about $60^{\circ}N$. Consequently, the difference between the measured and the required directions is 20°; it can be explained by minor local deviations of the strike of the fractures. In addition, it is necessary to consider that the two-dimensional model is based on an infinite extension in the third dimension. Actually, however, the plates with which the rock between the fissures is represented are of finite length and more or less rigidly clamped at one end, and possibly also at both ends. Therefore, a tilt component may appear perpendicular to the direction resulting from the fracturing.

4.3.4.5 Evaluation of the Model

The model, which is based on different thicknesses of the weathered layer, therefore, is compatible with the four fundamental pieces of information (see Section 4.3), which can be derived from the tilt measurements, and is correlated with precipitation. Therefore, it must be viewed as a probable model for the actual effective mechanism. It reproduces the behavior on a large scale correctly, but some restrictions with respect to the predictability have to be made because of the great simplifications. In particular, the representation of the fissured graywacke by a system of rock plates, which permits free mobility of the individual elements under the action of water level changes, must be mentioned here. Actually, the joints in general form no continuous cracks from the top edge of the graywacke to depths of 40 m, but a large number of smaller joints. These are interconnected,

set opposite each other, and interleaved; the fissures are partially filled. Moreover, the model representation should not lead to the impression that no mutual elastic coupling of the graywacke structure is present. This certainly must be considered in setting up the model calculations, in particular for this problem, but also for further model calculations (see Section 5.1.5).

4.3.5 GEOLOGICAL DISTURBANCES IN THE REGION OF THE STATION

The analytical solution for the tilt of a rock plate under one influence is, as Figure 4.7 shows, ambiguous; that is the measured tilts can be explained by different combinations of plate thickness and applied force. For an increasing thickness of the plate, the prerequisites for the analytical solution no longer are fulfilled, so that the calculation must be performed with other methods, such as, for example, the finite element methods.

As a supplement to the previous calculations, we will now investigate whether it is possible to model these effects by the bending or deformation of block-like structures with a width (elongation in the y-direction) of a few tens of meters to a few hundreds of meters and varying the height of the blocks and the areas of application of the force. For this we use a two-dimensional finite element model which is shown in Figure 4.11.

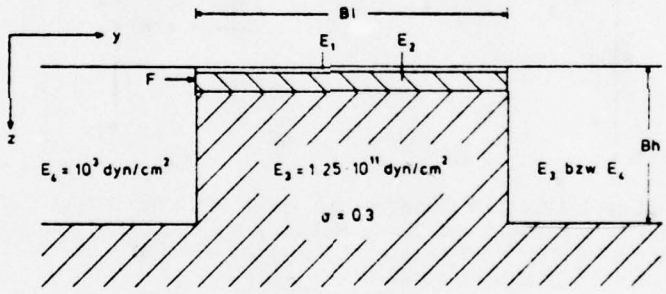


Figure 4.11. Sketch of the Model Used for the Finite Element Calculations (Bl = block length; Bh = block height; E = modulus of elasticity; σ = Poisson's ratio; F = applied force)

A section perpendicular to two geological bodies is modeled; the rock between them forms a block, the geometry of which is described by its height and width and which is connected below with the solid graywacke. The material properties used are identical with the values given in Table 5.4. The free mobility of the block in the y-direction is ensured by the fact that the modulus of elasticity outside of the block is smaller than that in the block by a factor of 10^8.

According to Section 4.1 the ratio of the tilt changes measured at depths of 15 m and 30 m is about 2:1. In order to reproduce this ratio with the postulated block structure the forces must act in a depth range of $0 \leq z \leq 10$ m as shown in Figure 4.12.

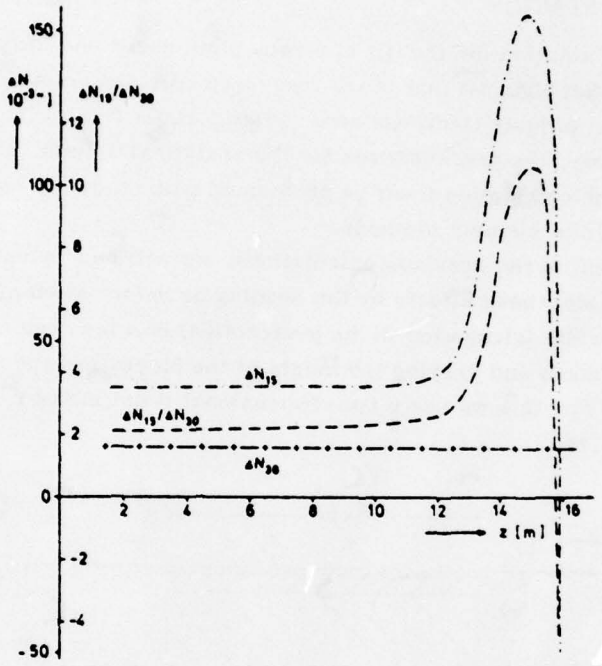


Figure 4.12. Tilt Changes at Depths of 15 m (ΔN_{15}) and 30 m (ΔN_{30}) and Their Ratio as a Function of the Depth in Which a Pressure Change $\Delta p = 0.981 \cdot 10^5$ dyn/cm^2 ($\hat{=}$ 1 m of water is present)

In the calculated example, the block height is 50 m and the length is 100 m. In order to investigate the dependence of the amplitude ratios and the absolute amplitudes on the block length, these values are calculated as a function of the block length, the point of application of the force being at a depth of 4 m. The equivalent forces which result from a pressure change of $1.962 \cdot 10^5$ dyn/cm^2 (Δp = 2 m of water) operate at this point. The results are presented in Figure 4.13 for the side of the block on which the forces act and show that a lower limit can be given for the block length, from which the amplitude ratio and the amplitudes themselves are well approximated; this limit is about 80 m. The dependence

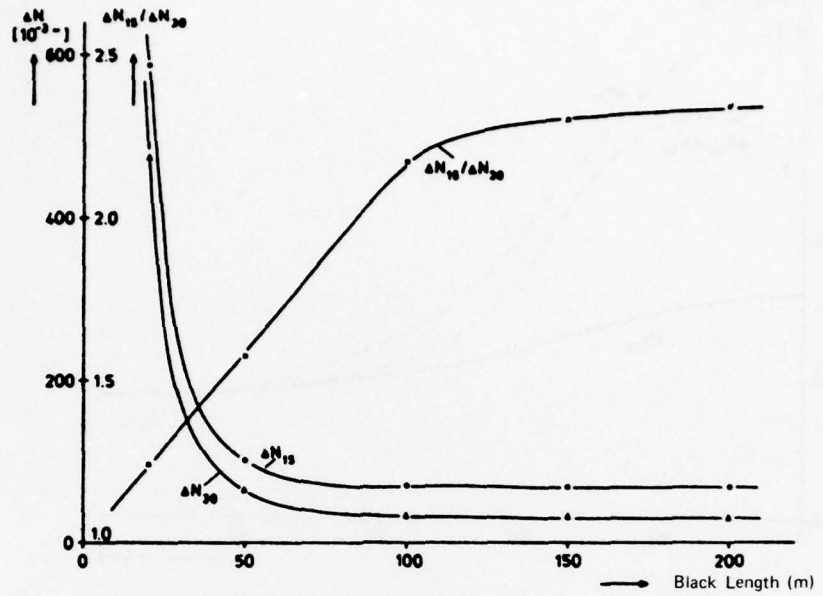


Figure 4.13. Tilt Changes at Depths of 15 m (ΔN_{15}) and 30 m (ΔN_{30}) and Their Ratio as a Function of The Block Length (block height = 50 m; pressure change ≙ 2 m of water)

on the block height is slight; changes of 10 m produce deviations in the result of only about 1 to 2 percent.

A block length exceeding this length produces no appreciable change in the given values, so that the model may be modified to the extent that only one geological parameter (that in which pressure changes which lead to a deformation of the surrounding rock appear as a result of a fluctuating water level) is required for explaining the measured effect. These deformations and the resulting tilts decrease, as Figure 4.14 shows, with increasing distance from the point of application of the force, especially at a depth of 15 m, so that the ratio of the tilts falls is less than 1.4 even at a distanceof 20 m.

Consequently, with respect to the position of the point of measurement relative to the assumed geological disturbance, it is necessary that the point be located within this 20 m. Since tilt changes in an easterly direction appear in the case of a pressure increase, the direction of the disturbance also is determined; a NS direction west of the station at a distance less than 20 m.

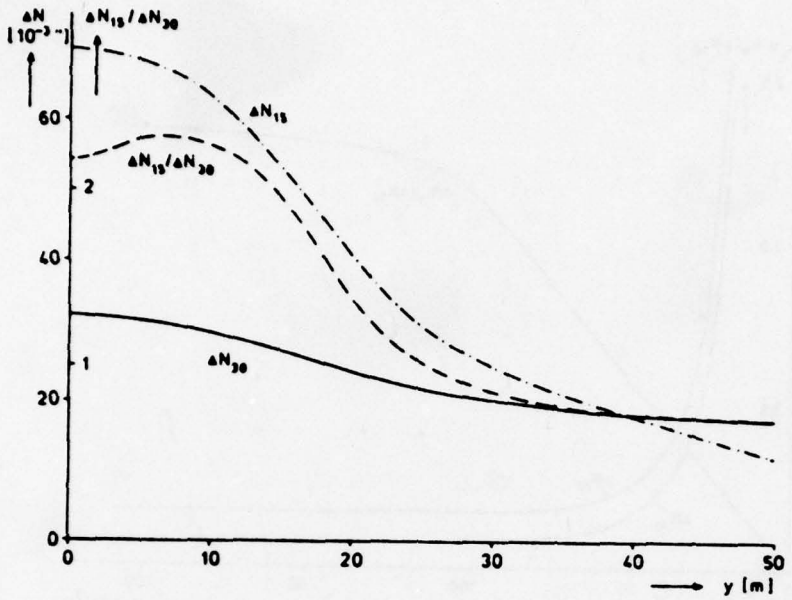


Figure 4.14. Tilt Changes at a Depth of 15 m (ΔN_{15}) and 30 m (ΔN_{30}) and Their Ratio as a Function of The Distance From the Left Edge of the Block (block height = 50 m; $\Delta p \hat{=} 2$ m of water)

Vein disturbances cannot be considered to be a cause (see Figure 5.11), since the vein ranges in the vicinity of the station have a strike of 110° and, moreover, lie essentially south of the station. There are no specific clues about further disturbances which fulfill the above mentioned criteria. Therefore it must be observed that the model discussed indeed is basically suitable for explaining the measured tilt effects, but cannot be reconciled with the known geological structures at the Zellerfeld-Mühlenhöhe Station.

4.4 Results and Consequences

On the basis of a comparison of the tilt recordings with the precipitation events in the corresponding period of time, it is established that, when the precipitation falls as rain, there is a clear correlation between the signal onsets. However, the time history of the tilt curve is not exclusively determined by the precipitation parameter. This is demonstrated in attempts to approximate the tilt signal with the use of this parameter. Other different model concepts show that a number of basically conceivable effective mechanisms can be excluded.

With a great deal of probability, the cause of the tilt signals lies in the tendency of the graywacke, in which the boreholes were made, to fracture. As a

consequence of precipitation or thawing periods, water fluctuations appear in the fracture system. The resulting forces create distortions of the rock between surfaces. This model also explains the difficulties which appear in the case of the prediction of the tilt signal by the precipitation. The pressure differences which appear between neighboring fissures are the dominant cause of the tilt changes. However, the ground moisture, the slope, and minor details of the topography also have an influence. The complicated interplay of these parameters, which are in part constant and in part variable over time, determines the actual effective pressure differences. It appears improbable that the individual parameters can be determined sufficiently precisely by measurements. The only reasonable possibility at the present time appears to be to measure the pressure differences themselves. This could be performed by recording the water fluctuations in several boreholes on two mutually perpendicular lines. The model would have to be checked with the use of these measurements. The problem of filtering the data would then have to be reconsidered.

Therefore, with respect to the future location of observation stations it must be concluded that the installation of tiltmeters in cracked rock such as that occurring at the Zellerfeld-Mühlenhöhe Station is to be avoided. In this case it does not matter if the tilt measurements are performed primarily for the purpose of making the most exact determination of the tide parameters possible or if geodynamic problems are the primary consideration. In both cases the signal-to-noise ratio is significantly impaired by the effects described.

Ideal conditions are found in uncracked, unlayered, completely homogeneous material in which there is no water flow. In general, these conditions are not fulfilled. However, investigations show that a considerable portion of the above-mentioned problems may be avoided if the boreholes for the installation of the tiltmeters are sunk in a region with a level topography and a layered subsoil with a horizontal bedding of the layers. Any asymmetry in the topography, the geology, or the elastic and physical rock parameters can lead to tilt effects which are eliminated only with great difficulty.

5. SECULAR TILTS

The existence of uninterrupted recordings, the length of which should be multiple of the longest period appearing in the recordings, is a prerequisite for the investigation of secular tilt effects (here secular tilt effects are to be understood as those signal components with periods greater than 100 days). Since this requirement, especially for measurements with horizontal pendulums, is difficult to fulfill, up to now little has been published about such effects. The studies by

Picha and Skaslky[42] are one of the few exceptions. They succeeded in decomposing the so-called variation curve into linear and periodic (annual and semi-annual) components. The interpretation of the annual component in terms of temperature fluctuations on the earth's surface for a measurement depth of 1009 m and the inference of a 20-year period from the linear portions appear very unreliable. Simon and Schneider,[25] on the basis of a year-long experience with horizontal pendulums, come to the conclusion that no information about the secular tilts of larger tectonic units can be obtained from the zero point variations of horizontal pendulums because of the influence of very local tectonic effects and instrumental and installation motion components.

Because of their considerably greater base length, strain meters make it possible to anticipate more reliable information about secular strain changes. The results of Berger and Wyatt[43] and of Berger and Levine[44] show that aperiodic strain changes of a reasonable order of magnitude are measured with these instruments. An annual component, which can be explained by thermoelastic distortions in the rock, is superimposed on the strain changes.

The tilt measurements at the Zellerfeld-Mühlenhöhe Station are particularly significant in this regard, since the uninterrupted recordings for a period of two and one-half years, available here for the first time, make is possible to perform a more detailed analysis of secular tilt effects on a vertical pendulum. The disadvantages caused by installation in mines are avoided by installation in boreholes. The longer base as compared with horizontal pendulums decreases the influence of local effects. Finally, surface effects, such as appear in the case of strain meters located immediately under the earth's surface, are diminished. In addition, observations at different depths offer a good possibility for monitoring the depth dependence of the measurement effect of the model developed.

Current interpretations of secular tilt effects in general rely on visual correlations, and, particularly, on the seasons. In general, model calculations are dispensed with, or the model is so simple (Berger[45]) that the results provide only rough guides for the interpretation (see Section 5.1.4).

First of all, in the analysis of the Clausthal data, the long-period portions in the tilt measurements are investigated with statistical methods such as correlation

---

42. Picha, J. and Skalsky, L. (1958) A contribution to the study of the zero point motion of the horizontal pendulum, Studia Geoph. et Geod. 2:243-260.

43. Berger, J. and Wyatt, F. (1973) Some observations of earth strain tide in California, Phil. Trans. R. Soc. London A274:267-277.

44. Berger, J. and Levine, J. (1974) The spectrum of earth strain from 10^{-8} to 10^{2} Hz, J. Geophys. Res. 79:1210-1214.

45. Berger, J. (1975) A note on thermoelastic strains and tilts, J. Geophys. Res. 80:274-277.

and regression analysis as well as maximum entropy spectral analysis. The results are interpreted in connection with previously published data about this region. Model calculations are carried out in order to monitor specific parameters by means of the evaluation of the measured data. Finally, the causes of the remaining aperiodic portions are discussed.

5.1 Annual Fluctuations in the Ground Temperature and Long-Period Tilts

5.1.1 PRELIMINARY EVALUATION IN THE TIME DOMAIN

Herbst[17, 46] gave the first indications of a connection between the ground temperature and the long-period tilt effects at the Zellerfeld-Mühlenhöhe Station. For the comprehensive quantitative investigations, one year of data were subjected to a preliminary evaluation. The recording of P3 (15 m depth) in the x-component, thus, in the original measurement direction (see Table 2.1), was chosen from the available material. Next, the tides were filtered out, and then the remaining short-period signal portions were eliminated with the use of binomial smoothing and a low-pass filter with a bell curve-like response (Holloway[47]), which had a cut-off frequency of 0.002 cph (corresponding to T = 500 h) in the case of a filter order of 128.* The aperiodic portions were considered to be linear and analyzed according to the least squares method. Filtering of the ground temperature data, which was measured once daily at a depth of 1 m at the Braunlage Weather Station, was not necessary. Namely, the measuring depth of 1 m already assured that the fluctuations of air temperature and the temperature of the surface layers were eliminated, and the measurements of the temperature and tilt had approximately the same frequency content.

The two time series are shown in Figure 5.1. The relative phase shift of 50 ± 5 days, by which the tilt lags behind the ground temperature has already been compensated for. We observe good agreement in amplitude between the measured curves at the dominant periods; the phase delay of 50 days indicates that temperature fluctuations at greater depths than 1 m are responsible for the tilt changes created.

This result of the preliminary evaluation shows that further analysis of this problem is worthwhile. In this case the evidence of annual periodicity for the

---

*The numerical filters mentioned in Section 5.1.2.2 were not yet available at the time of the preliminary evaluation.

46. Herbst, K. (1974) Correlation of Meteorological Effects and Pendulum Oscillations at the Zellerfeld-Mühlenhöhe Station, 34th Anniversary of the German Geophysical Society, Berlin. Central Office for Air and Space Documentation and Information ZLDI Conf. 74-016-002.

47. Holloway, P. L., Jr. (1958) Smoothing and filtering of time series and space fields, Advances in Geophysics 4:351-389.

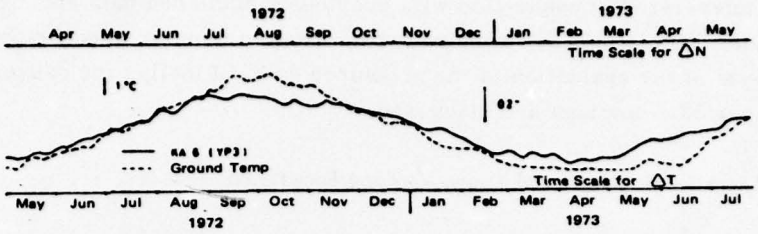


Figure 5.1. Comparison of Long-Period Tilt Components with the Annual Variation of the Ground Temperature

tiltmeter recording at a depth of 30 m is of particular significance for model developments. Figure 4.2 shows that visual correlation for the P1 data does not lead to the goal because of the unfavorable signal-to-noise ratio resulting from precipitation.

Therefore, the dominant frequencies in the recordings are next investigated with the use of the maximum entropy spectral analysis method, and then the amplitudes and phases are then determined by means of correlation and regression analysis.

5.1.2 SPECTRAL ANALYSIS OF TILT AND TEMPERATURE DATA WITH THE MAXIMUM ENTROPY METHOD

5.1.2.1 Characteristics of the Maximum Entropy Method (MEM)

The Blackman and Tuckey*[48] auto-correlation method and the periodogram method (squared Fourier spectrum) are conventional methods for evaluating the power spectrum of a random sample. Both methods operate with assumptions about the data outside of the interval to be analyzed. The calculation of the auto-power spectrum assumes a zero extension of the data in the case of the evaluation of the auto-correlation function; the calculation of the Fourier power spectrum is based on a periodic continuation of the data from $+\infty$ to $-\infty$, the fundamental period corresponding to the length of the data. In general, both assumptions are unrealistic. A further disadvantage is that the window function used in each case leads to a distortion of the power spectra. The accuracy of the two methods consequently is very low if the periods to be analyzed are comparable with the length of the data interval.

---

*[sic] should be Tukey.

48. Blackman, R.B. and Tuckey,* J.W. (1958) The Measurement of Power Spectra, Dover Publications Inc., New York.

These disadvantages are avoided with the maximum entropy method (MEM) (Lacoss,[49] Ulrych and Bishop[50]). In this case we are dealing with a spectral analysis technique which was developed especially for the analysis of short time series and which is characterized by the fact that no assumptions are made about the data outside of the interval under analysis or the information contained in the data.

Therefore, we have a data-adapted method which is configured to the actual noise characteristics of the random sample to be analyzed in a way such that the spectral density represents maximum entropy or maximum informational content for the random sample, and, nevertheless, is in complete agreement with the available data. Smylie, Clarke, and Ulrych[51] showed that the spectral density function S(f) satisfies these conditions and is given by

$$S(f) = \frac{P_{M+1}}{2 f_{Ny} \left| 1 + \sum_{j=1}^{M} \gamma_j e^{-i 2\pi f j \Delta t} \right|^2} \tag{5.1}$$

in which f_{Ny} is the Nyquist frequency. The constant P_{M+1}, the auto-correlation coefficients ϕ_j, and the coefficients of the prediction-error-operator γ_j satisfy the M + 1 normal equations

$$\begin{bmatrix} \phi_o & \phi_1 & \cdots & \phi_M \\ \phi_1 & \phi_o & & \phi_{M-1} \\ \vdots & & & \vdots \\ \phi_M & \phi_{M-1} & \cdots & \phi_o \end{bmatrix} \begin{bmatrix} 1 \\ \gamma_1 \\ \vdots \\ \gamma_M \end{bmatrix} = \begin{bmatrix} P_{M+1} \\ 0 \\ \vdots \\ 0 \end{bmatrix} \tag{5.2}$$

An optimum prediction filter operator Γ_M of the length M + 1 which is given by the sequence

$$\Gamma_M = \{1, \gamma_1, \ldots, \gamma_M\}$$

---

49. Lacoss, R.T. (1971) Data adaptive spectral analysis methods, Geophysics 36:661-675.

50. Ulrych, T.J. and Bishop, T.N. (1975) Maximum entropy spectral analysis and autoregressive decomposition, Reviews of Geophysics and Space Physics 13:185-200.

51. Smylie, D.E., Clarke, G.K.C., and Ulrych, T.J. (1973) Analysis of Irregularities in the Earth's Rotation, Methods in Computational Physics, Vol. 13, pp. 391-430, Academic Press, New York.

is determined by this system of normal equations. P_{M+1} is a constant which gives the average energy of the prediction error after using the prediction error filter of the length M + 1 and which is created by convolution of Γ_M with the auto-correlation coefficients of the random sample to be analyzed ϕ_o, ϕ_1, ..., ϕ_M in

$$P_{M+1} = \sum_{k=0}^{M} \gamma_k \phi(k)$$

The calculation of the maximum entropy spectrum of a discretized time function x_i, i = 1, N according to Equation (5.1) thus reduces to the calculation of the prediction error filter and the corresponding energy, which remains in the prediction error. According to Burg[52] Γ_M and P_{M+1} are determined recursively with the use of the Levinson algorithm. The length of the prediction-error-operator Γ_M is chosen according to Akaike's[53] criterion so that the prediction error

$$(FPE)_M = \left(\frac{N + M}{N - M}\right) F_M$$

becomes minimal, F_M being the average standard error of the prediction with the use of Γ_M (see Ulrych and Bishop[50]).

5.1.2.2 Spectral Analysis and its Results

The data from the years 1972 to 1974 are available for the calculation of the ME-spectra. These data are subjected to a successive filtering with the filters cited by Flach et al.[19] The use of the flattest low-pass filter with a cut-off period of around 120 days in the pass band produces the signals shown in Figure 5.2 which provide the basis for further calculations. For the entire period of time, the ground temperature, like the tilt data, is given at intervals of one day. According to Section 5.1.1 filtering is not necessary.

A first evaluation of the ME-spectra of these data shows that (in contrast to the opinion expressed by Ulrych and Bishop[50] that the first relative minimum of the prediction error determines the optimum length of the prediction error filter) a satisfactory resolving capacity is obtained only when the length of the prediction error filter is determined by the absolute minimum of the prediction error. In the analysis of test data (a composite of harmonic oscillations of different frequencies),

---

52. Burg, J. P. (1968) A New Analysis Technique for Time Series Data, Report for NATO Advance Study Institute on Signal Processing, Enschede.

53. Akaike, H. (1971) Autoregressive model fitting for control, Ann. Inst. Statist. Math. 23:163-180.

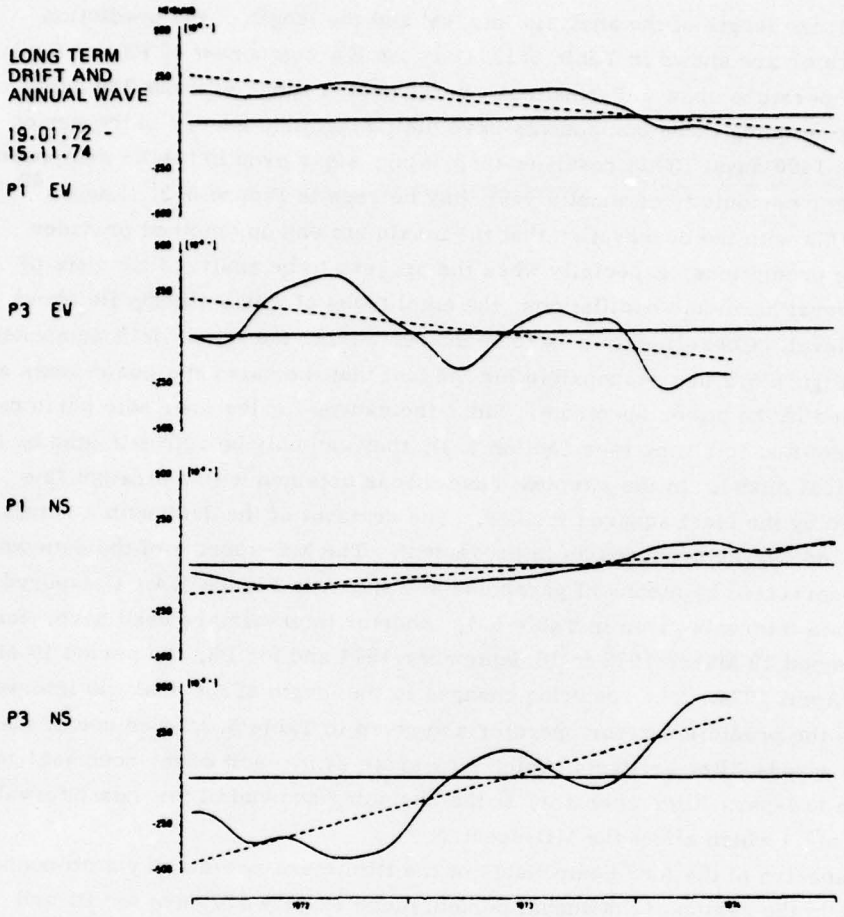


Figure 5.2. Tilt Changes in the Period Range over 120 Days for the EW and NS Components of P1 (installation depth 30 m) and P3 (installation depth 15 m); --- Linear Drift Component according to Flach et al[19]

however, the Akaike criterion modified by Ulrych and Bishop provides satisfactory results with respect to the resolving capacity and stability of the spectra. The following data about the length of the prediction error operator in each case refers to the absolute minimum of the prediction error which is calculated for the interval $M \leq N/2$. The spectral density function S(f) is calculated for discrete frequencies in the range $0 \leq f \leq 0.01$ cpd ($\hat{=}$ T = 100 d) at a step f = 0.000111 cpd.

The normalized maximum entropy spectra for the two components of the tiltmeters P1 and P3, as well as that of the ground temperature, are shown in

Figure 5.3; the length of the analysis interval and the length of the prediction error operator are shown in Table 5.1. Only the EW component of P3 and the ground temperature show a distinct peak in the period range of about 360 days, while the remaining three components have their maximum energy in the period range over 1400 days. This result is surprising, since even in the NS component of P3 a clear periodicity of about a year may be seen in Figure 5.2. Lacoss[49] refers to this with the observation that the maximum entropy method provides worthwhile predictions, especially when the process to be analyzed consists of one or several harmonic oscillations, the amplitudes of which clearly lie above the noise level. Consequently it is to be suspected that the linear drift components shown in Figure 5.2 are responsible for the fact that the harmonic components are not resolved in the power spectrum. Since the causes for the aperiodic portions are not known at this time (see Section 5.3), they can only be approximated by a mathematical model. In the simplest case this is obtained with a straight line determined by the least squares method. The removal of the drift with a parabola of the second degree produces an improvement. The ME-spectra of the data which are drift-corrected by means of parabolas are shown in Figure 5.4. Compared with the data intervals given in Table 5.1, shorter intervals are used here: for P1, the period 19 March 1972 to 16 September 1974 and for P3, the period 19 March 1972 to 1 April 1974. The resulting changes in the length of the analysis interval as well as the prediction error operator are given in Table 5.2. The use of these measures avoids filter artifacts (which may arise as a result of the renormalization of the low-pass filter operator) at the beginning and end of the data interval (Flach et al[19]) which affect the ME-spectra.

The spectra of the four components of the tiltmeters now display a pronounced maximum in the region of the annual period; more exactly 374 days for P1 and 360 days for P3. All other frequency components of the signal are highly attenuated, and, in fact, with the exception of the NS component of P1, they are reduced to 10 percent of the amplitude of the annual tilt variation. The width of the peak is the least for the instrument recording at a depth of 15 m, since at this depth the signal-to-noise ratio is the most favorable at the annual periods.

The information which results from the use of the maximum entropy spectral analysis technique may be summarized to the effect that the method is basically a suitable means of providing unquestionable proof of annual variations in the available measurement data with a recording length of 2-1/2 to 3 years, if the following conditions are fulfilled:

(1) The length of the absolute minimum of prediction filter is to be used for determining the length of the prediction filter.

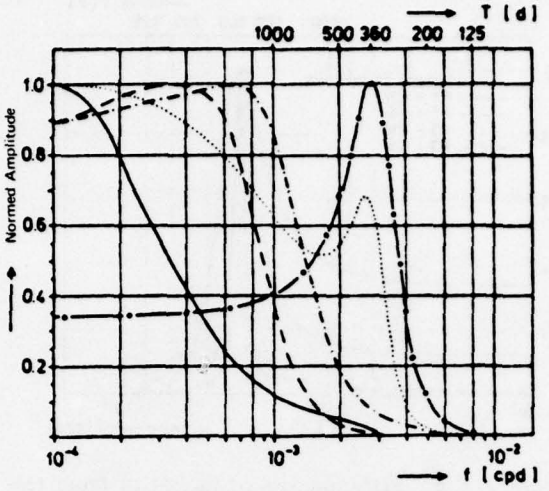


Figure 5.3. ME-Spectra of the Tilts from the Four Tiltmeter Components in the Period Range over 120 Days and of the Ground Temperature Measured at a Depth of 1 m (-o-o = ground temperature; - - - - = EW-P1; ——— = NS-P1; . . . . . = EW-P3; - · - · - = NS-P3)

Table 5.1. Length of the Analysis Intervals and the Prediction-Error-Operators

Tiltmeter		Length of the Analysis Interval [α]	Length of the Prediction-Error-Operator [α]
P1	EW	1032	62
	NS	1032	50
P3	EW	864	37
	NS	864	56
Ground Temperature		1032	42

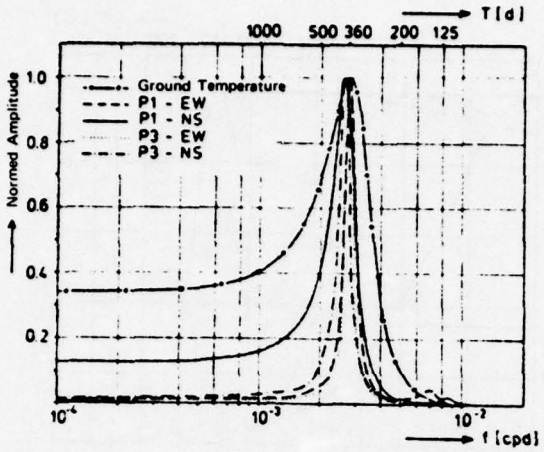


Figure 5.4. ME-Spectra of the Tilts from the Four Tiltmeter Components After Drift Elimination and of the Ground Temperature at a Depth of 1 m

Table 5.2. Length of the Analysis Intervals and of the Prediction Error-Operators After Drift Removal (see Figure 5.4)

Tiltmeter		Length of the Analysis Interval [α]	Length of the Prediction-Error-Operator [α]
P1	EW	912	71
	NS	912	54
P3	EW	744	61
	NS	744	57

(2) Aperiodic components in the signal to be analyzed must be satisfactorily eliminated.

The calculated ME-spectra must be checked for stability in relation to the data interval, since frequency shifts may appear because of perturbations in the observed data, such as those caused by filter artifacts.

5.1.3 AMPLITUDE AND PHASE DETERMINATIONS

According to Lacoss,[49] calculation of the amplitudes from the maximum entropy spectra is possible when the process being analyzed displays small peaks in the frequency domain. In this case, the power which is to be assigned to the corresponding frequency is given by the area under the peak. The integration for determining the area is carried out for the ME-spectra shown in Figure 5.4 over the frequency range from $1.5 \cdot 10^{-3}$ cps $\leq f \leq 5 \cdot 10^{-3}$ cpd. The results presented in Table 5.3 are given, with account having been taken of the normalization factors.

Table 5.3. Results of the Amplitude and Phase Calculations

Component		Amplitude [10^{-3}"] According to MEM	P1/P3	Amplitude [10^{-3}"] According to Regression Analysis	P1/P3	Phase [d]
EW	P1	24.5	1:5.1	31.6 ± 7.3	1:5.4	28
	P3	124.8		170.6 ± 26.7		10
NS	P1	25.8	1:4.4	21.5 ± 9.8	1:8.1	30
	P3	113.3		173.5 ± 15.1		80

This method of amplitude determination has not been extensively tested on real data so far, so that no predictions can be made about the reliability of the calculated amplitudes. The same data are subjected to a correlation and regression analysis in order to check their reliability; the mutual phase relationship also is obtained in this way. The MEM cannot provide this, since, according to the relationships cited in Section 5.1.2.1, the coefficients of the prediction error filter are determined with the auto-correlation function, in the calculation of which phase information is lost.

The correlation and regression analysis are accomplished by calculating the cross-correlation function for the ground temperature and the two components of tiltmeters P1 and P3. The regression coefficient and its confidence interval for an error probability of 5 percent are calculated for the time lag at which the cross-correlation function reaches its maximum. The calculations are performed taking account of the auto-correlation in the statistical testing of correlations between two time sequences (Taubenheim[54]). From these values and from the

54. Taubenheim, J. (1974) Taking account of the autocorrelation in checking the statistical significance of correlations between two time series, Gerlands Beitr. Geophysik 83:413-416.

amplitude of the annual temperature wave at a depth of 1 m of ± 5.8°C we then obtain the amplitudes of the annual tilts. The results are given in Table 5.3, the phases representing the time lag (days) of the tilt with respect to the ground temperature.

Comparison of the amplitudes shows that for tiltmeter P1 the amplitudes determined with MEM are included in the error range of the amplitudes calculated with regression analysis. For tiltmeter P3 the amplitudes calculated with MEM lie about 13 to 28 percent under the lower error limit determined from the regression analysis. These comparatively small deviations are, however, negligible for the following model considerations.

5.1.4 MODEL CONSIDERATIONS

The investigations up to now have shown that a connection between the annual variation of the ground temperature and the tilt changes with annual periods may be viewed as probable. However, these results, which rely on statistical methods, must also be supported by model representations which are numerically verifiable.

In this case the models have to be set up so that we are dealing with a variable factor which is connected with the annual temperature wave, which displays a depth dependence according to Table 5.3, and, moreover, is of the order of magnitude of the absolute tilt amplitudes. Further, the model must be compatible with the calculated phases.

First, the measured tilt effects may be produced by temperature fluctuations in the vicinity of the tiltmeters which are determined by the heat conductivity of the rock, the casing of the borehole, and the column of air located in it. The solution of the heat conduction equation for a homogeneous half-space makes it possible to perform an evaluation of the temperature fluctuations to be expected. According to this, for a thermal conductivity of 10^{-2} cm^2/sec, at a depth of 15 m there are fluctuations of about ±0.07°C, and about ±0.0006°C at a depth of 30 m; that is, the amplitude ratio amounts of about 100:1. These small temperature fluctuations therefore cannot be detected with the temperature measurements conducted in the borehole. The phase difference between the two can be estimated as being around 9 months. Even when we consider that the distortion from the borehole leads to a reduction in the amplitude ratio and a reduction in the phase difference, we see that the values for the amplitude ratio and the phases presented in Table 5.3 are not attained. Therefore, this model is not capable of explaining the measured effects.

Another model concept is based on temperature fluctuations near the earth's surface and the volume changes connected with them. Under appropriate circumstances these may lead to considerable tilt and strain changes and are manifested at great depths. This effect, in general called the thermoelastic effect, has been

treated phenomenologically, for example by Benioff[55] as well as by Berger and Wyatt.[43] The analytical solution for the simple model of an infinitely extended elastic half-space, on the surface of which a temperature wave propagates, is given by Berger.[45] The relationships derived there are next used here in order to check whether this model is compatible with the results from the Zellerfeld-Mühlenhöhe Station with respect to the annual tilt variations. In this case we see that with an appropriate choice of the parameters, such as, for example, horizontal wavelength and depth penetration of the temperature of the wave, the results for one of the measurement depths are always realizable. However, it was not possible to produce the tilt amplitudes measured at depths of 15 and 30 m with the same parameters. For the development of further model representations, it follows that, in order to maintain the proper order of magnitude generally, horizontal wavelengths of around 100 m must be assumed. Temperature fluctuations of this spatial extent are indeed conceivable, but appear to be quite hypothetical. Moreover, another difficulty is that their amplitude is considerably smaller than that of the annual temperature wave.

From the results of these analytical considerations it must be concluded that the model of a homogeneous half-space is not suited to the complexity of the actual relationships. Model calculations on a larger scale, for example, those which consider the topography and the geological structures, however, cannot be carried out analytically. Therefore, we will use the finite element method below in order to determine whether the measured tilt effects can be interpreted as thermoelastic distortions in the rock in connection with the topography and geology.

5.1.5 MODEL CALCULATIONS FOR THERMOELASTIC DISTORTIONS IN THE BEDROCK WITH THE FINITE ELEMENT METHOD

5.1.5.1 The Topographic Model of the Zellerfeld-Mühlenhöhe Station

The goal of the following investigations is to acquire an idea of the order of magnitude of the thermoelastic effect caused by the topography. This is based on a two dimensional finite element model in the East-West direction through the Zellerfeld-Mühlenhöhe Station, which is shown in Figure 5.5.

The geometry of the elements is chosen so that the nodal point spacing in the region of the borehole ($y = 0$) is relatively close and becomes larger toward the edge of the model, which is bounded at $y = +1000$ m or $y = -1000$ m and $z = 1000$ m. The boundary conditions are chosen so that the nodes which border the sides of the model have a degree of freedom in the z-direction and are fixed in the y-direction; the nodes bordering the model below are freely movable in the y-direction and fixed in the z-direction.

55. Benioff, H. (1959) Fused-quartz extensiometer for secular, tidal and seismic strains, Bull. Geol. Soc. Am. 70:1019-1032.

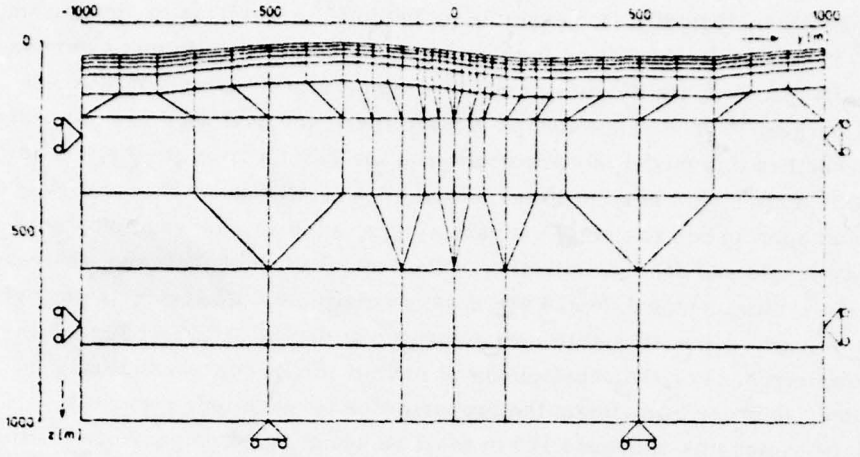


Figure 5.5. Two Dimensional Finite Element Model of the Zellerfeld-Mühlenhöhe Station (EW direction)

The geological information in the vicinity of the station is based on that encountered in sinking the boreholes. Thus, a three-layer situation can be assumed. The upper layer of about 2 m in thickness is formed by unconsolidated material. This is followed by a 6 m thick layer of weathered graywacke, with solid graywacke down to a depth of 1000 m under this. It is assumed that the two upper layers are uniform over the entire length of the model and run parallel to the earth's surface.

The model parameters are summarized in Table 5.4. In part, they are based on measurements, and in part on published sources. The compressional wave velocities determined by Slomka, [56] which were obtained with the hammer method, are used for determining the elastic properties of the three materials. The thermal parameters are taken from the literature (Landolt-Börnstein, [57] Kohlrausch[58]). The temperature-depth distribution may be calculated as a function of time from the solution of the heat conduction equation. For a thermal conductivity of 10^{-2} cm^2/s and an annual temperature wave amplitude of $\pm 8^{\circ}C$, we obtain the set of curves given in Figure 5.6; it is given for a half year with time intervals of ten days. These functions are obtained for an entire year by reflection

56. Slomka, T. (1974) Seismic Investigations with a Digital Apparatus, Diploma Study at the Inst. f. Geophysik, TU Clausthal (unpublished).

57. Landolt-Börnstein (1952) Volume III: Astronomy and Geophysics, Springer, Berlin-Göttingen-Heidelberg.

58. Kohlrausch, F. (1962) Practical Physics, B. G. Teubner Publishing Company, Stuttgart.

Table 5.4. Summary of the Model Parameters

Material	Depth [m]	Compression Wave Velocity [m/sec]	Poisson's Ratio	Density [g cm^{-3}]	Modulus of Elasticity [dyne/cm^2]	Coefficient of Linear Expansion [deg^{-1}]
Surficial Layer	0-2	500	0.3	1.7	$1.14 \cdot 10^9$	10^{-5}
Weathered Graywacke	2-8	2000	0.3	2.0	$2.85 \cdot 10^{10}$	10^{-5}
Solid Graywacke	8-1000	4000	0.3	2.3	$1.25 \cdot 10^{11}$	10^{-5}

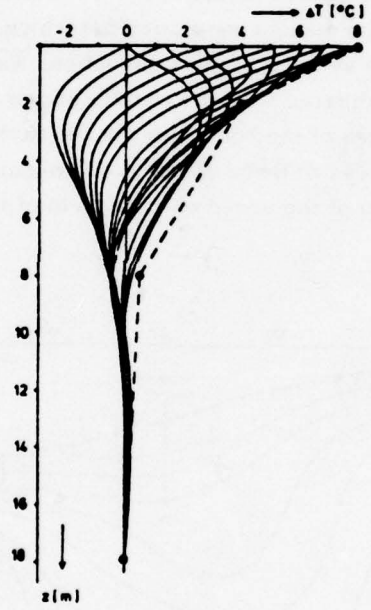


Figure 5.6. Approximation of the Temperature Distribution with Depth with the Use of the Temperature-Depth Functions Calculated at Ten-Day Intervals (——— = calculated temperature-depth functions (thermal conductivity 10^{-2} cm^2/sec) · = nodal point temperatures between which temperatures are linearly interpolated)

about the z-axis. The maximum temperature changes at each depth are thus given by the envelope of this family of curves; this is approximated by the dashed curve. From these then we have the temperatures at the upper four nodal point levels in Figure 5.5. This choice of approximation provides for an evaluation of the maximum tilt effect, since the tilts at different depths increase proportionally to the temperature changes and are at a maximum when the temperatures at all nodal points, between which the temperature is interpolated linearly, have the same sign.

5.1.5.2 Discussion of the Results of the Model Calculations

The result of the numerical analysis with the parameters given in Section 5.1.5.1 is presented in Figure 5.7 in the form of a cross-section with lines of equal tilt change. The representation is limited to the region of the model in which the tilt measurements are carried out and in which it is possible to conclude that the geometry of the model and the boundary conditions have an insignificant effect on the calculations. Another model, the elements of which have the same geometry in the region of the measuring station but which is three times as long in the y-direction and twice as deep in the z-direction, was calculated for a control. The deviations as compared with the results shown in Figure 5.7 are at most 10 percent in the region of the borehole; the tilt variations of the larger model are this much in excess of those of the given model. This variation is negligible for the evaluation of the order of magnitude of the thermoelastic effect.

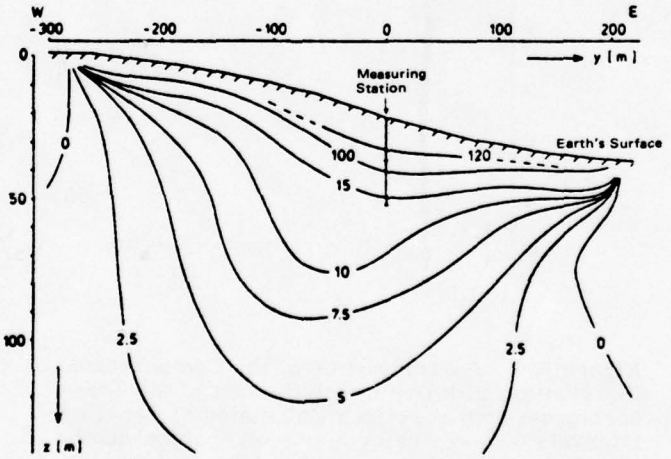


Figure 5.7. Cross-Section with Lines of Equal (Maximum) Tilt Changes (in 10^{-3}") Which Result from the Annual Variation of the Ground Temperature

For clarity the representations of the tilt changes in the upper layers is dispensed with. The maximum tilt changes lie in the region of the greatest slope in the topography (approximately 10 percent) and for the surficial layer amount to about 3 ", and about 1" for the underlying layer of weathered graywacke.

Figure 5.7 contains two essential pieces of information. With respect to the tilt measurements at the Zellerfeld-Mühlenhöhe Station it shows that the tilt changes calculated at depths of 15 m and 30 m of about $110 \cdot 10^{-3}$" and $14 \cdot 10^{-3}$" represent a good approximation to the value measured for the EW direction (see Table 5.3). If we also add the 10 percent tilt change from model influences and use a value of $1.2 \cdot 10^{-5}/^{\circ}C$ for the thermoexpansion coefficients instead of a value of $1 \cdot 10^{-5}/^{\circ}C$ (uncertainty of this parameter: at least ±20 percent), the agreement is improved, and the values determined with model calculations are within the limits of error of the amplitudes determined from the measured values for the EW component. In the case of P1, the calculated value approaches 30 percent of the lower error limit. This proves that the thermoelastic effects connected with the topography in the immediate vicinity of the station represent a plausible explanation for the tilts of annual periodicity.

Moreover, these model calculations provide basic information for the installation of tiltmeters. Tilt measurements in sloping topography are very questionable (the model calculated here has a maximum slope of only 10 percent) if the tiltmeters have a cover between 0 and 8 m thick, especially if recent tectonic movements are to be determined from measurements with recording times of a few months. Because of the great influence of annual ground temperature waves, serious misinterpretations are possible here. Regions in which the land is level, or hilltops or depressions if measurements are to be made in hilly country, are particularly suited for the installation of tiltmeters. As Figure 5.7 shows, the tilt changes in the region of the hilltop and the depression are minimal and independent of the depth (the lines with zero tilt variation run approximately vertically). However, the cover over the tiltmeters should also amount to about 10 m in these places; otherwise, minor shifts of the measuring point in the y-direction may lead to considerable changes in the tilt effects.

Therefore, we see that Berger's conclusion (drawn from model calculations), that is, a significant damping of the thermoelastic effect is not possible with a reasonably obtained amount of cover because of the proportionality between horizontal wavelength and penetration depth, cannot be confirmed here. At the Zellerfeld-Mühlenhöhe Station, the assumption of temperature fluctuations in the ground with spatial wavelengths of several 100 km for the annual variation is not suitable for explaining the measured effects. The tilt effects possibly caused in this way apparently are negligible. Quite clearly the thermoelastic distortions coupled with the topography are dominant. The resulting tilts may be taken as

smaller than $2 \cdot 10^{-3}$" for the annual temperature wave at a depth of about 10 m and a topographically appropriate choice of the measuring point.

5.1.5.3 Sensitivity of the Results to Variations in the Model Parameters

The model parameters presented in Section 5.1.5.1 are known with different degrees of certainty. The compressional wave velocities are the most reliable. A reduction of 35 percent in the velocities given in Table 5.4, with the other parameters remaining constant, however, results only in an increase in the tilt effect of at most 2 percent; the choice of the compressional wave velocities, and, thus the determination of the moduli of elasticity, is not critical. The model reacts to variations in the Poisson's ratio, σ, significantly more sensitively. In the case of the model under consideration, the transition from $\sigma = 0.30$ to $\sigma = 0.25$ leads to a reduction of the tilts of about 10 percent at a depth of 15 m and a maximum of 5 percent at a depth of 30 m. In this case a minor change in the depth dependence of the tilts also appears. These changes refer to the region of the model in which the boreholes are located.

The literature contains no data about the linear expansion coefficient α of the surficial layer because it is highly variable with respect to material composition, and, moreover, it is subject to great fluctuations resulting from the variation of the water saturation of the rock. However, the model calculations show that the result only insignificantly depends on the magnitude of the expansion coefficient in the surficial layer. The transition from $\alpha = 10^{-5}/^{o}C$ to $\alpha = 0/^{o}C$ creates tilt changes smaller than 2 percent at the measurement depths. This also indicates that the temperature distribution in the top layer has no influence worth mentioning for the tilt changes at depths of 15 m and 30 m. The increase in the modulus of elasticity by a factor of 100 upon the transition from the surficial layer to the solid graywacke is responsible for the rapid decrease of tilt with depth.

The selected form of the temperature approximation may be used for evaluating possible tilt effects. However, no statements can be made about the phase relation between the temperature behavior and tilt changes at the two measuring depths. In the first place, this is due to the element dimensions in the upper 20 m of the model. In order to be able to obtain a definitive answer about the phases, it would be necessary to discretize the temperature depth distributions for different times, at intervals of at least 1 m. This would lead to an element length in the z-direction of 1 m, since the temperature changes can be given only at the nodal points. Therefore, the dynamic analysis would be simulated by several static analyses in which the temperature-depth distribution is given at different times. These very comprehensive calculations could not be performed within the framework of this study.

5.2 Other Effects with an Annual Periodicity

A model which is in good agreement with the measurements was developed in Section 5.1.5 for the tilts with an annual period. Further possible influencing factors which vary with annual periods are discussed below.

These include, among other things, atmospheric air pressure fluctuations; their amplitude may be given as ±2.5 mb from the long-term monthly average values of the air pressure for Clausthal-Zellerfeld. The resulting tilt effect is of the order of magnitude of $\pm 0.5 \cdot 10^{-3}$" according to the estimates made in Section 3.3; that is, the tilt effect is too small by a factor of about 100. Together with the considerations of the depth dependence of the tilt effect in the case of large area pressure fluctuations (see Section 3.3.2.4), it follows from this that a connection between the measured annual tilt components and the annual air pressure wave is to be excluded.

The long-term average values of precipitation for Clausthal-Zellerfeld (Climatology of the German Reich[59]) indeed display a slight annual periodicity; however, a period of 6 months is significantly more prominent. Since these periods do not appear in the tilt measurements, no connection should exist between precipitation and tilts at annual periods. The fracture model discussed in Section 4.3.4 shows, moreover, that the required amplitude ratio of the tilts at depths of 15 and 30 m of about 6:1 cannot be simulated with this model.

Since a number of ponds and reservoirs are located in the region of the Oberharz, it is necessary to determine how much their annual water level fluctuations may influence the tilt measurements. Stadtweger Pond, which is around 800 m from the station, is the closest pond to the station (see Figure 2.1). The loading effect created by it is calculated as a function of the distance for a water level fluctuation of 3 m. The deformation component calculated with the finite element method is shown in Figure 5.8. Since the attraction component (see Section 3.3.3) is negligible for the distance of 800 m, the loading effect at a distance of 800 m can be given as $\pm 3 \cdot 10^{-3}$". This result is practically insensitive to variations of the elastic properties of the subsoil for the given distance range. According to Section 3.3.2.4, the depth dependence of the deformation component is negligible at distances of around five times the radius of the loaded surface. The measured depth dependence is not compatible with this. The comparison of the tilts for the Y-component of P3 with the water level of Stadtweger Pond (see Figure 5.9) in part does indeed show a good correlation; such marked phases as filling of the pond to its maximum level, however, are not reflected in the given tilt components. The fact that the tilt resulting from the filling of the pond does not take place in the direction of the loading also argues against this concept.

---

59. Climatology of the German Reich (1939) Bietrich Reimer Press, Berlin.

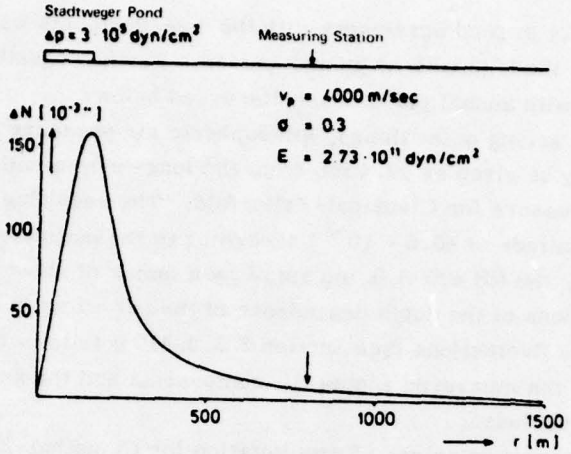


Figure 5.8. Vertical Tilt Variations ΔN in the Case of Loading from Water Level Fluctuations in Stadtweger Pond as a Function of the Distance r (model of a homogeneous plane half-space)

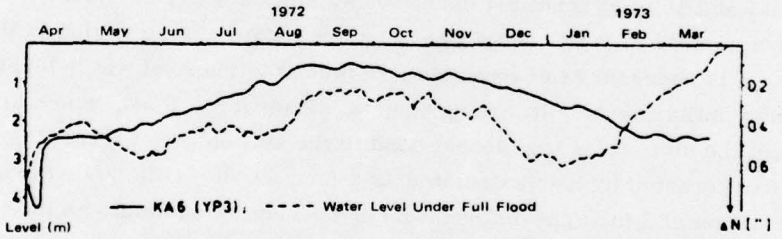


Figure 5.9. Comparison of the Annual Tilt Variations of YP3 with the Water Level Fluctuations in Stadtweger Pond

The same considerations hold true for water level fluctuations at the Okertal Dam. At the Zellerfeld-Mühlenhöhe Station, water level fluctuations of 5 m should create tilt effects of about $\pm 0.5 \cdot 10^{-3}$".

In summary it can be stated that none of the factors discussed in this section is capable of explaining the measured annual tilt variations. The given orders of magnitude in each case are to be understood as estimates of the maximum tilt effect possible. This means that these effects are completely negligible for the annual tilt variations (about $\pm 170 \cdot 10^{-3}$") measured at a depth of 15 m. On the other hand, the abovementioned influences are noticeably superimposed on the

tilts created by thermoelastic distortions at a depth of 30 m. This explains why, for example, in the time series in Figure 5.2, the annual periodicity is not so easily recognized as in the case of tiltmeter P1. In addition, these effects may be partially responsible for the differences between the measured tilt amplitudes and those calculated for the thermoelastic effect.

5.3 Aperiodic Portions of the Signal

5.3.1 COMPOSITION OF THE LONG-TERM DRIFT

Among other reasons, tiltmeters are installed for the purpose of detecting recent movements of the earth's crust. A meaningful interpretation of the measurements, however, is possible only if instrument effects or effects due to the local tectonics of the installation site are successfully separated from the tilts of larger tectonic units. Previously this problem could not be solved for tiltmeters. According to the view of Simon and Schneider[25] cited at the beginning of Section 5, horizontal pendulums are not suited to this problem. Up to now there has been little information available about vertical pendulums. Because of the recording time of about 3 years at the Zellerfeld-Mühlenhöhe Station, some contribution to this problem might be possible here. The first results were presented by Flach et al[19]; these results are reviewed and supplemented below.

With the use of the maximum entropy method in Section 5.1.2.2, it is shown that the process can be used successfully only if the aperiodic portions (in the following also called drift) can be eliminated. This also includes long-period portions which are presented as aperiodic because of the short recording length. Since no assumptions can be made about the long-term drift and possible tectonically caused portions, an optimally adapted mathematical model must be used for approximating the aperiodic components. First the sum of least squares is used as a criterion for optimum matching, and then the quality of the maximum entropy spectra; that is, the attenuation of the noise at periods greater than a year and the sharpness of the peak at this period. The best results here are provided by approximation with a parabola of the second order; that is, this drift model is viewed as the most probable one.

Figure 5.10 gives the result of the drift approximation in the form of a two-dimensional representation for both tiltmeters P1 and P3; the two curves describe the motion of the tiltmeters in their respective measurement planes.

A definitive interpretation of these curves by exclusively tectonically caused tilts is not possible. The preferred direction of tilt between 30° and 60°, which lies approximately perpendicular to the strike of the Oberharz range of veins (see Figure 5.11), argues in favor of such components. According to Hinze,[23] the rock sections between the vein disturbances, the extent of which lies between a few hundred meters and a few kilometers, sink gradually; vertical displacements

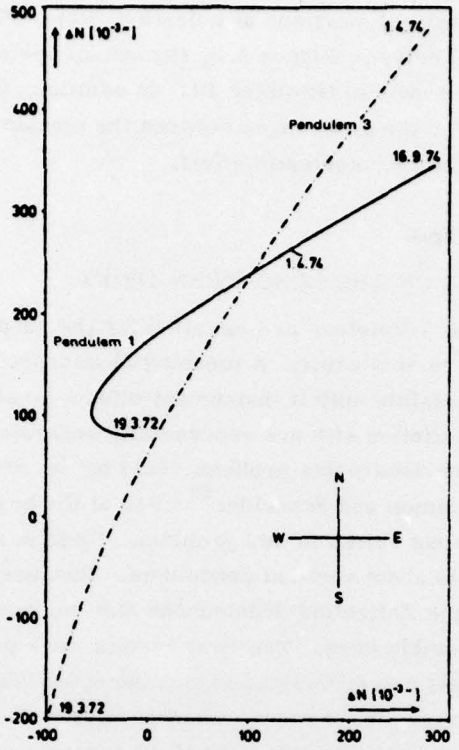


Figure 5.10. Aperiodic Portions of the Drift in the Case of Approximation with a Parabola of the Second Order for P1 and P3 (installation depths: P1 = 30 m; P3 = 15 m)

of 300m to 500 m appeared at the Bockswiese-Festenburg-Schulenberger range of veins which lies about 3 km northeast of the Zellerfeld-Mühlenhöhe Station. Therefore, it may be suspected that a portion of the measured tilts, which cannot be specified more closely at the present time, is created by these tectonic processes.

Different reasons may be responsible for the different drift behavior of the two pendulums, both in direction and in amplitude. Figure 5.10 shows that the drift of the instrument installed at a depth of 15 m is two to three times greater than that of the tiltmeter recording at a depth of 30 m. From this it may be concluded that the tectonically caused portions of the tilt have superimposed upon them an effect which clearly decreases with depth, such as, for example, secular temperature changes in the ground which may arise from climate changes. In

THIS PAGE IS BEST QUALITY PRACTICABLE
FROM COPY FURNISHED TO DDC

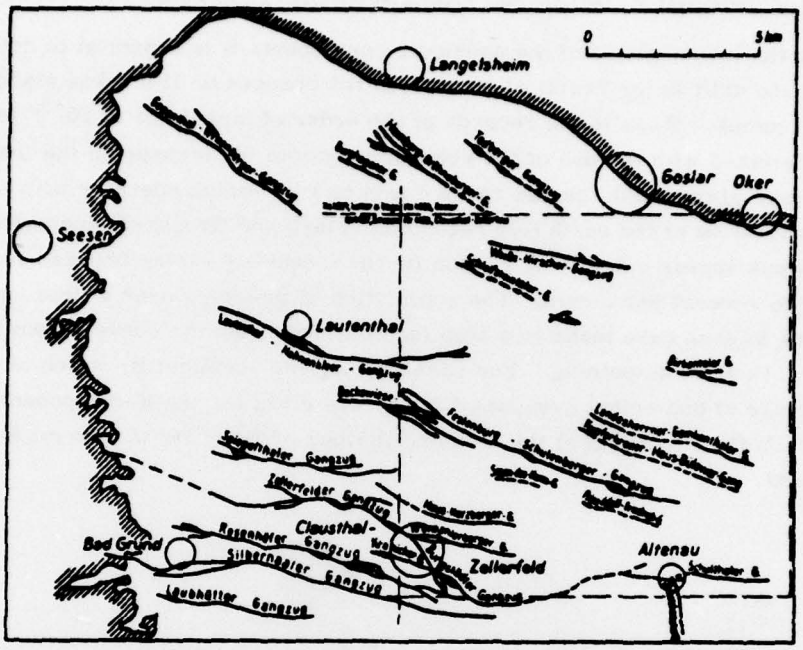


Figure 5.11. Survey of the Most Important Veins and Ranges of Veins in the Northwestern Oberharz (according to Hinze[23])

addition, it is conceivable that the geology of the immediate vicinity of the station may create a similar effect because of the immediate proximity of the Haus-Herzberger range of veins. The accompanying disturbances of this range of veins may modify the previously described tilt effects in the two boreholes in different ways. Finally, the marked disturbance in the drift pattern which appeared in 1972 indicates that we have to reckon with the influence of portions of the drift caused by the instruments or the borehole itself.

These considerations show that an unambiguous interpretation of the aperiodic tilt components fails not so much because of the relatively short recording time, but more because of the lack of comparable recordings. Both tiltmeters measure the rock section in which the tectonic movements are suspected in the same place, but not with reference to the measurement depth and proximity to the Haus-Herzberger range of veins and its accompanying disturbances. The evaluation of the data obtained at the Clausthal-Feldgraben Station may produce further information about this complex problem.

5.3.2 POSSIBLE ORIGIN OF THE APERIODIC COMPONENTS

For the investigation of the aperiodic components it is essential to determine whether the drift is the result of continuous tilt changes or if it takes place in discrete jumps. Steps in the records of the order of magnitude of 10^{-5}" to 10^{-4}" can be detected with the use of the recording system for measuring the free oscillations of the earth (period range 1 min to 1 h), which operates with a gain of 41 db relative to the earth tide recording (Flach and Grosse-Brauckmann[60]). These steps appear completely randomly; the frequency varies between several per day to several per month. The summation of the steps over a time interval of a week in each case leads to a step function which has the curve shown in Figure 5.12 after smoothing. For comparison, the secular tilt, which is derived with the use of numerical low-pass filters, are given for the X-component (see Table 2.1); the recording of the free oscillations of the earth is also made in this component.

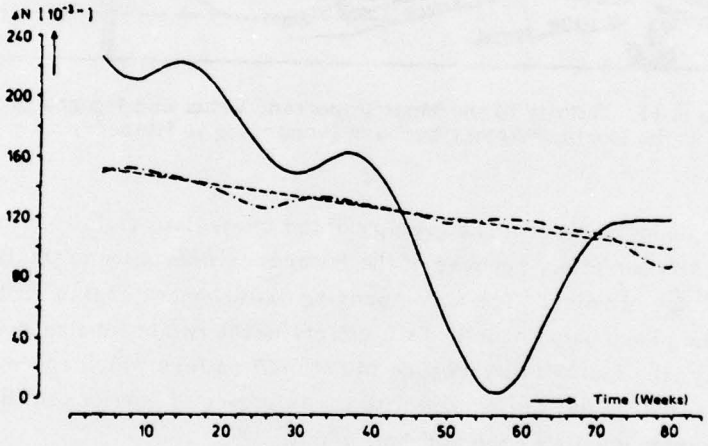


Figure 5.12. Comparison of the Long and Aperiodic Tilt Components Separated by Numerical Filtering (——) with the Component Calculated by Summation of the Steps (-.-.) as Well as Its Linear Portion (-----) During the Period 20 January 1974 to 20 July 1975 for the X-Component of P1

60. Flach, D. and Grosse-Brauckmann, W. (1974) An electronic filter and damping system for the Askania borehole tiltmeter, J. Geophys. Res. 41: 303-310.

Comparison of the two curves shows that the drift resulting from the summation of the steps agrees in trend with the drift derived with numerical filtering; that is, the steps provide a significant contribution to the total drift. The drift component caused by the steps may be viewed as linear to a good approximation. The slightly periodic character is not correlated with the periodic portions of the curve determined by filtering.

This comparison, carried out for one component of course, establishes no generally valid conclusions; however, it provides some hints for future studies. In the first place, microearthquakes, for example in the region of the Bockswiese-Festenburg-Schulenberger range of veins, are conceivable as a cause of the recorded jumps; that is, the subsidence of the rock section, described in Section 5.3.1, proceeds in discrete jumps. The seismicity of the Oberharz would have to be monitored by several seismic stations in order to verify this idea. This would make it possible to determine if such tremors exist at all and, if so, where they are localized. The recordings for measuring the free oscillations of the earth would have to be set up with adequate time resolution so that a reliable correlation between the seismic signals and the tilt measurements would be possible.

However, effects of a local character also are conceivable. Thus, irreversible displacements of the borehole may occur, perhaps after great mechanical stressing of the casing, for example, by strong surface waves during earthquakes. Furthermore, it is possible to imagine corrosion effects in the housing of the vertical pendulum which might possibly cause abrupt tilts as a result of very small changes in the position of the expansion pin ($<10^{-8}$ cm). Whether these effects are borehole- or equipment-specific may be determined by the comparison of two Askania borehole tiltmeters, each of which is equipped with a recording system for detecting earthquakes. In order to obtain an unambiguous interpretation, the equipment must record at the same depth and it must be ascertained that the two boreholes are sunk into the same geological unit. According to whether or not the jumps are correlated, in time it can be determined whether they are the result of local or equipment-caused effects, or if they are connected with the regional geological structures.

6. SUMMARY

The tilt recordings from two Askania borehole tiltmeters operating at depths of 15 m and 30 m were investigated at periods longer than those of the tides. Continuous recordings for a period of two and a half years (1972 to 1974) were available for this purpose. The first goal of the investigations was to attempt

to obtain qualitative information about the influence of the factors considered on the tilt measurements by means of simple methods, such as the comparison of signals between which a connection is suspected during the time period. Then if a connection could be viewed as probable or certain, statistical and deterministic methods were used for the purpose of obtaining a quantitative description. These results formed the basis for the development of model representations which, as far as possible, were supported by model calculations. In this case it was basically a matter of calculating static displacements in an elastic medium under the influence of variable forces, for example, as a result of variable pressure distributions or thermally induced expansion processes.

With regard to the influence of large-area atmospheric pressure fluctuations, the investigations led to the result that it was not possible to demonstrate tilt changes caused by air pressure for the Zellerfeld-Mühlenhöhe Station. Evaluation of the deformational component for the model of a homogeneous half-space and the calculation of the attraction effect showed that such an influence would not be expected, since the maximum possible tilts which would appear in the case of air pressure fluctuations of 50 mb would be smaller than $10 \cdot 10^{-3}$". However, a comparison of the local air pressure variations with the measured tilts showed that the amount actually present in the measurements was smaller.

The dominant tilt signals in the period range of several days were caused by the penetration of water into the ground. In general this took place upon the occurrence of precipitation in the form of rain and during melting periods. The connection between the amount of precipitation and tilt could not be described by a linear system; the prediction of the tilt signal using the parameter "amount of precipitation per unit time" required for filtering the recordings also could not be achieved with the desired accuracy. The discussion of different model representations showed that the measured tilt changes could not be explained by

- thermoelastic distortions in the rock as a consequence of temperature fluctuations which appeared as a result of the heat transfer by the precipitation;
- swelling effects of clay materials in the case of water absorption;
- loading effects from the precipitation;
- water level fluctuations in a geologically disturbed or weak zone.

A model satisfying the measurements in all respects was based on the fractured nature of the graywacke in which the boreholes were sunk. A downslope increasing thickness of the weathered layer created lateral fluctuations in the fracture water level. The resulting pressure differences in adjacent fractures or fracture systems led to elastic bending of the rock structures laying between them, and thus to tilts. In spite of the great simplifications upon which this model was based it closely approximates the measurements. It was in good agreement with

the observed values for the amplitudes at different depths and for the amplitude ratio and with the preferential direction and duration of the signal.

The long-period components in the tilt measurements could be identified with the use of the maximum entropy method as tilt variations taking place with annual periodicity. Model calculations with the finite element method showed that they were caused by the annual ground temperature wave. The temperature fluctuations connected with this created a strain in the subsoil, which in the case of the Zellerfeld-Mühlenhöhe Station led to tilts (strain-induced effect) coupled with the undulating topography. Other effects also appearing with annual periodicity were negligibly small as compared with the thermoelastic effects.

At the present time, it is not possible to separate the aperiodic portions into equipment- or borehole-specific portions and possible tectonically caused tilts. The results of this study, however, make it appear worthwhile to investigate the presence of seismically active zones in the region of the Oberharz Culm folded zone in connection with its seismicity. In this way it might be possible to obtain reliable information about recent tectonic processes in this region. The tilt measurements at the Clausthal-Feldgraben Station can also provide an important contribution to this.

The investigations carried out within the framework of this study show that the signal components recorded in the period range above that of the tides at the Zellerfeld-Mühlenhöhe Station essentially are caused by precipitation and long-period temperature variations. Tilts caused by precipitation influence the signal-to-noise ratio unfavorably, to the extent that at the present time an investigation of tilts caused by air pressure is not possible. Such investigations appear to offer little promise, even in the future, since the tilt signals caused by precipitation cannot be separated with sufficient accuracy.

Therefore, to sum up, it may be stated that in the first place the local geological structures and topography in the immediate vicinity of the station are mirrored in the tilt measurements in this period range carried out at the Zellerfeld-Mühlenhöhe Station. In this regard the results of this study quite clearly differ from those of previous studies. It is to be assumed that this is not due to the design and the particular location of the Zellerfeld-Mühlenhöhe Station. In comparable investigations at other stations, features appearing in addition to the tides frequently have been interpreted as extensive elastic deformations and tectonic crustal movements without having the problem of possible local factors investigated more closely.

The investigations also have illustrated the problems involved in separating a specific effect from tilt signals and correcting the measured tilts. This is particularly evident in the case of the investigation of the tilts resulting from precipitation. Even with the very comprehensive modeling of this phenomenon

used here, it remains extremely uncertain whether the signal can be quantitatively simulated with models or predicted with suitable transfer functions. To be sure, advances can be obtained with a significant increase in the experimental and technical expenditure; however, it appears doubtful (if, for example, the model of the fissured graywacke as a cause of the tilt changes should be confirmed) if a sufficient separation of the signals created in this way is possible. It should not be possible to determine the geometry of the fracture system to the extent necessary for model calculations either by geological or geophysical means. Difficulties in determining the elastic, petrophysical, and thermal model parameters are involved here.

The experience obtained here is of significance for the future construction of observatories. The selection of the measuring location should be preceded by a detailed study of the topography, geology, and hydrology of the neighborhood of the station in order to be able to evaluate the possibilities of the appearance of disturbing effects. Since the influence of the immediate surroundings of stations on the tilt measurements has not been investigated for the majority of stations, investigations of this type should again be carried out for each station, taking account of experience to date. Only then should an interpretation of the data with respect to tectonic processes be carried out. Therefore, it is recommended that in the future, measurements be carried out in regions in which the subsoil is well known geologically and hydrologically and, moreover, is of simple structure. In this way the probability of largely disturbance-free measurements is increased considerably, and disturbances which still appear can be more easily dealt with in numerical model calculations. While, the investigation of such disturbing effects is, to be sure, very interesting from a scientific point of view, the primary goal of the tilt measurements is to find the solution of large-scale* geodynamic problems in connection with other natural sciences. The present study should provide a contribution to the preliminary studies required for this.

*Underlined in original manuscript.

References

1. Lennon, G.W. and Baker, T.F. (1973) Earth tides and their place in geophysics, Phil. Trans. R. Soc., London A274:199-202.
2. Bachem, H.C. (1973) The Upper Limit of Accuracy of Earth Tide Readings with Horizontal Pendulums Taking Account of Local Tectonic Disturbances, Diss. TU, Hannover.
3. Bonatz, M. and Rocholl, W. (1973) The Total Evaluation of the Measurement Data Obtained with Horizontal Pendulums in the Erpel Test Station in 1965-1971, Mitt. Inst. Theor. Geod., Bonn.
4. Grosse-Brauckmann, W. (1976) High Precision Ball Calibration of the Askania Borehole Tiltmeter, Proceedings of the 7th Int. Symposium on Earth Tides, Gyuala Szadeczky-Kardose ed., Schweitzerbart's Publishers, Stuttgart.
5. Wenzel, H.-G. (1975) Interpolation of true values for earth tide recordings by means of prediction filtering, Deutsche Geodät. Komm. B211:15-23.
6. Harrison, J.C. (1976) Cavity and topographic effects in tilt and strain measurement, J. Geophys. Res. 81:319-328.
7. Harrison, J.C. (1976) Tilt observations in the Poorman Mine near Boulder, Colorado, J. Geophys. Res. 81:329-336.
8. Farrell, W.E. (1972) Deformation of the earth by surface loads, Reviews of Geophysics and Space Physics 10:761-797.
9. Levine, J. and Harrison, J.C. (1976) Earth tide measurements in the Poorman Mine, near Boulder, Colorado, J. Geophys. Res. 81:2543-2555.
10. Berger, J. and Beaumont, C. (1975) An analysis of tidal strain observations from the United States of America - I. The homogeneous tide, Bull. Seis. Soc. Am. 65:1613-1629.
11. King, G.C.P. and Bilham, R.G. (1973) Tidal tilt measurement in Europe, Nature 243:74-75.
12. Lettau, H. (1937) Plumb bob oscillations under the influence of tidal and atmospheric forces, Gerlands Beitr. Geophysik 51:250-269.

13. Lettau, H. (1940) Meteorologically caused crustal deformations and their detection by means of horizontal pendulum recordings, Forschungen und Fortschritte 21(16th Anniversary):223-224.

14. Tomaschek, R. (1959) Oscillations of tectonic blocks as a result of barometric load changes, Freiberger Forschungshefte C 60:35-55.

15. Simon, D. (1968) Contributions to the correction of clinometric and gravimetric tide recordings, Mitt. Inst. Theor. Physik u. Geophysik d. Bergakad. Freiberg 51.

16. Tanaka, T. (1969) Study on meteorological and tidal influences upon ground deformations, Spec. Contrib. Geophys. Inst. Kyoto Univ. 9:29-90.

17. Herbst, K. (1973) Meteorological Influences on Tilt Measurements at the Zellerfeld-Münlenhöhe Testing Station, Graduate Work at the Institute for Geophysics, TU Clausthal (unpublished).

18. Zschau, J. (1974) Pendulum Anomalies in Earth Tides – Recordings with the Askania Borehole Pendulum Designed by A. Graf, Diss. Univ. Kiel.

19. Flach, D., Grosse-Brauckmann, W., Herbst, K., Jentzsch, G., and Rosenbach, O. (1975) Results of long-term recordings with Askania borehole tiltmeters – Comparative analysis with respect to the tide parameters and long-period portions and instrumental investigations, Deutsche Geodät. Komm. B211:72-95.

20. Flach, D. and Rosenbach, O. (1971) The Askania borehole tiltmeter (tide pendulum) of A. Graf at the Zellerfeld-Mühlenhöhe testing station, Bull. Inf. Mar. Terr. 60:2934-2943.

21. Flach, D., Rosenbach, O., and Wilhelm, H. (1971) Investigations of A. Graf's Askania borehole tiltmeter (tide pendulum) at the Zellerfeld-Mühlenhöhe testing station, Bull. Inf. Mar. Terr. 60:2944-2954.

22. Mohr, K. (1973) Western Part of the Harz – A Collection of Geological Guides 58, Borntraeger, Berlin-Stuttgart.

23. Hinze, C. (1971) Legend for Clausthal-Zellerfeld Paper No. 4128 (Geological Map of Niedersachsen 1:25,000), Nieder Sachsen Office for Geological Research, Hannover.

24. Simon, D. and Schneider, M. (1967) The appearance of air pressure-induced distortions in horizontal pendulum readings at three different earth tide stations, Bull. Inf. Mar. Terr. 49:2218-2225.

25. Simon, D. and Schneider, M. (1973) Analysis of the nonperiodic ground deformations at the Tiefenort Tidal Station 1958-1973, Geodät. Geophys. Veröff. Series III.

26. Simon, D. (1975) Coherence of Tidal Parameters Observed at Tiefenort (GDR) with Respect to Pseudo-Tidal Effects induced by Atmospheric Pressure Variations, Report presented to the XVI General Meeting of the IUGG, Grenoble.

27. Boussinesq, J. (1885) Application of the Potential to the Study of the Equilibrium and the Movement of Elastic Solids, Gauthier-Villars, Paris.

28. Zienkiewicz, O.C. (1971) The Finite Element Method in Engineering Science, McGraw-Hill, London.

29. Beaumont, C. and Lambert, A. (1972) Crustal structure from surface load tilts, using a finite element model, Geophys. J. Roy. Astrom. Soc. 29:203-206.

30. Bathe, K.-J., Wilson, E.L., and Peterson, F.E. (1973) SAP IV – A Structural Analysis Program of Static and Dynamic Response of Linear Systems, Report No. EERS 73-11, Earthquake Engineering Research Center, University of California, Berkeley.

31. Slichter, L.B., and Caputo, M. (1960) Deformation of an earth model by surface pressures, J. Geophys. Res. 65:4151-4156.

32. Bullen, K.E. (1947) An Introduction to the Theory of Seismology, Cambridge Univ. Press.

33. Fortak, H. (1971) Meteorology, Carl Habel Publishers, Berlin and Darmstadt.

34. Götze, H.-J. (1976) A Numerical Procedure for Calculating the Gravimetric and Magnetic Field Values for Three-dimensional Models, Diss. TU Clausthal.

35. Kanasewich, E.R. (1973) Time Sequence Analysis in Geophysics, The University of Alberta Press.

36. Villwock, R. (1966) Industrial Geology, Stein Press, Offenbach/Main.

37. Philipsborn, H. von (1967) Tables for Identifying Minerals According to External Geological Features, E. Schweizerbart's Publishing Company, Stuttgart.

38. Betechtin, A.G. (1968) Lehrbuch der speziellen Mineralogie, VEB Deutscher Verlag für Grundstoffindustrie, Leipzig.

39. Grim, R.E. (1953) Clay Minerology, McGraw-Hill, New York.

40. Macke, W. (1967) Particle Mechanics – Systems and Continua, Academic Publishing Company Geest & Portig, Leipzig.

41. Schneider, H. (1973) Water Development, Vulcan-Verlag, Essen.

42. Picha, J. and Skalsky, L. (1958) A contribution to the study of the zero point motion of the horizontal pendulum, Studia Geoph. et Geod. 2:243-260.

43. Berger, J. and Wyatt, F. (1973) Some observations of earth strain tide in California, Phil. Trans. R. Soc. London A274:267-277.

44. Berger, J. and Levine, J. (1974) The spectrum of earth strain from 10^{-8} to 10^{2} Hz, J. Geophys. Res. 79:1210-1214.

45. Berger, J. (1975) A note on thermoelastic strains and tilts, J. Geophys. Res. 80:274-277.

46. Herbst, K. (1974) Correlation of Meteorological Effects and Pendulum Oscillations at the Zellerfeld-Mühlenhöhe Station, 34th Anniversary of the German Geophysical Society, Berlin. Central Office for Air and Space Documentation and Information ZLDI Conf. 74-016-002.

47. Holloway, P.L., Jr. (1958) Smoothing and filtering of time series and space fields, Advances in Geophysics 4:351-389.

48. Blackman, R.B. and Tuckey,* J.W. (1958) The Measurement of Power Spectra, Dover Publications Inc., New York.

49. Lacoss, R.T. (1971) Data adaptive spectral analysis methods, Geophysics 36:661-675.

50. Ulrych, T.J. and Bishop, T.N. (1975) Maximum entropy spectral analysis and autoregressive decomposition, Reviews of Geophysics and Space Physics 13:185-200.

51. Smylie, D.E., Clarke, G.K.C., and Ulrych, T.J. (1973) Analysis of Irregularities in the Earth's Rotation, Methods in Computational Physics, Vol. 13, pp. 391-430, Academic Press, New York.

52. Burg, J.P. (1968) A New Analysis Technique for Time Series Data, Report for NATO Advance Study Institute on Signal Processing, Enschede.

53. Akaike, H. (1971) Autoregressive model fitting for control, Ann. Inst. Statist. Math. 23:163-180.

*[sic] should be Tukey.

54. Taubenheim, J. (1974) Taking account of the autocorrelation in checking the statistical significance of correlations between two time series, Gerlands Beitr. Geophysik 83:413-416.

55. Benioff, H. (1959) Fused-quartz extensometer for secular, tidal and seismic strains, Bull. Geol. Soc. Am. 70:1019-1032.

56. Slomka, T. (1974) Seismic Investigations with a Digital Apparatus, Diploma Study at the Inst. f. Geophysik, TU Clausthal (unpublished).

57. Landolt-Börnstein (1952) Volume III: Astronomy and Geophysics, Springer, Berlin-Göttingen-Heidelberg.

58. Kohlrausch, F. (1962) Practical Physics, B. G. Teubner Publishing Company, Stuttgart.

59. Climatology of the German Reich (1939) Dietrich Reimer Press, Berlin.

60. Flach, D. and Grosse-Brauckmann, W. (1974) An electronic filter and damping system for the Askania borehole tiltmeter, J. Geophys. Res. 41: 303-310.

Biography

I was born on 8 October 1946 in Sachsenburg/Sachsen, the son of the salesman Felix Herbst and his wife Margarete, nee Müller.

1953-1957	Attended the grammar school in Lutter am Bbge.
1957-1966	Attended the modern language and natural science Seesen Gymnasium (modern language branch). Graduated 22 February 1966.
1966-1968	Army
1968-1973	Geophysical studies and Clausthal TU Preliminary exams: 12 October 1970 Final Exams: 2 November 1973

Since November 1973 I have been a doctoral candidate at the Institute for Geophysics of the Clausthal Technical University.